Technical Report
TR-18-06
April 2019

Paleoclimatic inversion of temperature profiles from deep boreholes at Forsmark and Laxemar

Volker Rath
Jan Sundberg
Jens-Ove Näslund
Lillemor Claesson Liljedahl

SVENSK KÄRNBRÄNSLEHANTERING AB

SWEDISH NUCLEAR FUEL
AND WASTE MANAGEMENT CO

Box 3091, SE-169 03 Solna
Phone +46 8 459 84 00
skb.se

SVENSK KÄRNBRÄNSLEHANTERING

ISSN 1404-0344
SKB TR-18-06
ID 1689569
April 2019

Paleoclimatic inversion of temperature profiles from deep boreholes at Forsmark and Laxemar

Volker Rath
Dublin Institute for Advanced Studies

Jan Sundberg
Chalmers University of Technology/JK Innova AB

Jens-Ove Näslund, Lillemor Claesson Liljedahl
Svensk Kärnbränslehantering AB

Preface

The following report constitutes a study reconstructing paleotemperatures from borehole thermal data at the Forsmark and Laxemar sites by inverse modelling. The study was initiated and managed by Assoc. Prof. Jens-Ove Näslund (SKB) and Dr. Jan Sundberg, Chalmers university of Technology. The modelling was performed by Dr. Volker Rath, Dublin Institute for Advanced Studies.

The results will be used, together with other published scientific information, for assessing the long-term safety of the planned and existing repositories for nuclear waste in Sweden (the spent nuclear fuel repository for long-lived high level waste, SFR for short-lived low- and intermediate level waste, and SFL for long-lived low-level waste).

The report manuscript was reviewed by Dr. Dmitry Demezhko, Institute of Geophysics, Russian Academy of Sciences, Yekaterinburg, Russia and Prof. Lars O Ericsson, Chalmers university of Technology, Göteborg, Sweden.

Stockholm, May 2019

Jens-Ove Näslund
Research coordinator Climate Programme SKB

Summary

This report presents inversions of borehole temperature profiles in boreholes at the Forsmark and Laxemar sites. Past changes in ground surface temperatures can be estimated from recent borehole temperature profiles, using numerical inversion methods. Here, we present results from a study using Bayesian methods for this task, which seek not only to derive one optimal model, but to characterize the full a posteriori probability density function of the parameters involved. In particular, we use Markov Chain Monte Carlo (MCMC) technique on a parameter vector combining a fixed number of step functions for temperature and the heat flow density at the base of the investigated borehole.

For Forsmark, an approximately 800–1 000 m deep averaged temperature profile was constructed by merging data from 8 different boreholes. It was combined with averaged rock properties and used for the inverse modelling of paleoclimate. In addition, simplified inverse modelling was also made using temperature logs from two selected Forsmark boreholes representing two groups of fundamentally different developments of local environmental conditions. For Laxemar we only present results for the single deepest borehole (KLX02).

The paleoclimate interpretation using the averaged merged temperature profiles were challenging, as the inversion results do not directly comply to our prior conception of the deglaciation, subsequent water cover, and modern climate. However, it was possible to identify significant differences between the two sites. From a climatological point of view, as expected, the presence of water cover is the dominant effect at both sites. From 11 kyr BP or 14 kyr BP, for Forsmark and Laxemar, respectively, GST (Ground Surface Temperature) appear to have been between 0 °C and +4 °C until 3 kyr BP, with slightly warmer conditions (3–4 °C) at the former site and colder (near 0 °C) at the latter site. The difference in the GSTHs (Ground Surface Temperature Histories) for both sites may be related to the position with respect to the coastline and the particular hydrological and environmental conditions met.

When using temperature data from the two selected individual Forsmark boreholes, with known different environmental histories, the ground surface temperature histories derived from the boreholes were more consistent with environmental conditions. These results tentatively suggests that the climate at Forsmark site during the Medieval warm period (around 1 kyr BP) was around +8 °C, that is 2–3 degrees warmer than at present. For the last 500 yr, the results agree well with proxy reconstructions as Luterbacher et al. (2004), if an appropriate SAT-GST correction is applied (Surface Air Temperature – Ground Surface Temperature).

Uncertainty in interpretation mainly derives from the unknown environmental regime (water temperature and salinity) controlling the ground surface temperatures during periods of shallow estuarine water cover. Uncertainty was also derived from the use of averaged compound temperature profiles and thermal conductivity data. The results of the study show that the individual historical paleoclimate development for borehole locations, within a larger site, may be fundamentally different, in turn affecting modelled paleoclimate histories.

The joint MCMC estimations of GSTH, heat flow density, and internal heat production rate also delivers most probable basal heat flow values (4 000 m depth), which are 49 mW/m^2 for Forsmark and 47 mW/m^2 for Laxemar (KLX02), respectively. These results support the former estimates of Sundberg et al. (2009).

Sammanfattning

Denna rapport presenterar rekonstruktioner av paleoklimat baserat på temperaturprofiler i borrhål i Forsmark och Laxemar. Historiska förändringar i markytans temperatur kan beräknas från uppmätta temperaturprofiler i borrhål med hjälp av numeriska inversionsmetoder. Här presenterar vi resultat från en studie som med hjälp av bayesianska metoder inte enbart syftar till att ta fram en optimal rekonstruktion av paleoklimat, utan även att karakterisera den fulla sannolikhetsfunktionen hos de involverade parametrarna. I synnerhet använder vi Markov Chain Monte Carlo-teknik (MCMC) på en parametervektor som kombinerar ett fast antal stegfunktioner för marktemperatur och värmeflöde i berget.

För Forsmark konstruerades först en genomsnittlig temperaturprofil ner till ett djup på cirka 800–1 000 m genom sammanslagning av temperaturdata från 8 olika borrhål. Denna kombinerades med medelvärden för bergets termiska egenskaper och användes för inversmodellering. Dessutom gjordes förenklad inversmodellering genom användning av individuella temperaturloggar från två utvalda borrhål (KFM01A och KFM02A) i Forsmark. Borrhålen valdes ut för att representera två grupper av borrhål med fundamentalt olika utveckling av lokala klimatförhållanden (orsakade av olika långa perioder av post-glaciala havstäckta förhållanden). För Laxemar presenterar vi endast resultat för det enskilt djupaste borrhålet (KLX02).

Den paleoklimatologiska tolkningen från de sammanslagna temperaturprofilerna var utmanande, eftersom inversionsresultaten inte var kompatibla med övrig information om deglaciation, efterföljande havstäckta period och Holocent klimat. Det var emellertid möjligt att identifiera signifikanta skillnader mellan de två platserna. Ur klimatologisk synvinkel var det som förväntat längden på den postglaciala perioden med havstäckta förhållanden som utgör den dominerande mekanismen på båda platserna. Från 11 kyr BP och 14 kyr BP, för Forsmark respektive Laxemar, verkar markytans temperatur (GST) ha varit mellan 0 °C och +4 °C till 3 kyr BP, med något varmare förhållanden (3–4 °C) vid Forsmark och kallare (nära 0 °C) vid Laxemar. Skillnaden i markytans temperaturhistoria (GSTH) mellan platserna kan vara relaterad till borrhålens position med avseende på kusten och de särskilda hydrologiska och miljömässiga förhållandena.

När man istället använder temperaturdata från de två utvalda individuella borrhålen i Forsmark, med olika miljöhistorik, var markytans rekonstruerade temperaturhistorier från borrhålen mer överensstämmande med den kända historiken för platsen. Dessa resultat föreslår att årsmedeltemperaturen i luften i Forsmark var omkring +8 °C under den medeltida varmperioden (omkring 1 kyr BP), vilket är 2–3 grader varmare än idag. För de senaste 500 åren överensstämmer resultaten väl med proxyrekonstruktioner av temperatur, om en korrigering tillämpas mellan lufttemperaturen nära markytan och markytans temperatur (SAT-GST-korrigering).

Osäkerhet i tolkningarna härrör huvudsakligen från okända miljöförhållanden (i huvudsak vattentemperatur och salthalt) som kontrollerar markytans temperatur under perioder av grunda vattenförhållanden. Osäkerhet konstaterades också från användningen av de sammanvägda temperaturprofilerna och vid användning av medelvärden för värmeledningsförmågan. Resultaten av studien visar att temperaturutvecklingen för individuella borrhålsplatser, inom en större plats, kan vara fundamentalt annorlunda, vilket i sin tur påverkar den modellerade paleoklimatologiska historiken. Resultaten visar därför också att det kan vara bättre att använda data från individuella borrhål vid den här typen av rekonstruktioner än att väga samman data från flera borrhål, speciellt om de senare har förväntat olika postglacial historik.

MCMC beräkningarna av markytans temperaturhistoria, värmeflöde och intern värmeproduktion ger också de mest pålitliga värdena för det basala värmeflödet (4 000 m djup). Resultaten visar att detta värmeflöde är 49 mW/m^2 för Forsmark och 47 mW/m^2 för Laxemar. Dessa resultat stöder de tidigare beräkningarna av värmeflöde från de två platserna presenterade i Sundberg et al. (2009).

Contents

1 Introduction

1.1 Background and purpose

Swedish Nuclear Fuel and Waste Management Company (SKB) is responsible for the management of spent nuclear fuel and radioactive waste generated within Sweden. SKB is planning to build a geological repository for spent nuclear fuel at the Forsmark site. An important document in the license application for building the spent nuclear fuel repository was an assessment of long-term repository safety. In this assessment, a range of climate scenarios form the basis for the assessment of long-term safety (SKB 2010, 2011). The same apply for e.g. the last safety assessment performed for the existing low- and intermediate level waste repository SFR (SKB 2014a, b). In addition, large site investigation programmes have been performed at the Forsmark and Laxemar sites and the final site descriptive models are summarized in SKB (2008, 2009).

The reference SKB climate scenario used in the safety assessments is based on a reconstruction of last glacial cycle climate- and environmental conditions. The purpose of the present study is to derive local climate information for the past thousands of years. The information will be used for improving the description of the climate of this period in the reference climate scenario, and to assess the temperatures previously used for the period. The results will be used in this way for all three repositories (the planned spent nuclear fuel repository for long-lived high level waste, the existing SFR repository for short-lived low- and intermediate level waste, and the planned SFL repository for long-lived low-level waste).

1.2 Ground surface temperature from borehole temperatures

Some of the safety assessment climate scenarios make use of paleoclimate information for the last glacial cycle and the Holocene. In this context, locally derived paleoclimate information is of importance, if available, since it describes the development specifically at the site of interest. Paleo-temperatures of the ground surface can be inverted from subsurface temperature logs in boreholes. The surface temperature of the Earth is controlled by the heat transfer across the ground-atmosphere interface. It is affected by climatic conditions, type of ground surface, vegetation and thermal properties of the subsurface.

Ground surface temperatures (GSTs) vary on many different time scales, ranging from diurnal and annual cycles to as long as glacial cycles (around 100 kyr). Temperature variations at the ground surface propagate downward and attenuate in the subsurface bedrock medium as a diffusion signal. The daily variation extends to 0.5–1.0 m depth, the annual variation to 10–20 m, decadal and millennial variations to tens and hundreds of metres, and glacial cycle variations down to several kilometres. The subsurface can therefore be utilized as a memory of past ground surface temperatures which can be extracted from borehole temperature data with forward and inverse modelling. Due to the diffusive character of the temperature signal, high-frequency information is efficiently low-pass filtered and the remaining data is useful for revealing long-term trends in ground surface temperature history. High-frequency variations can be studied through other palaeoclimate proxies, such as tree rings, ice cores, and lacustrine and marine sediments. In contrast to these often-used proxies applied in paleoclimate studies, the geothermal method does not require a translation from a proxy parameter to temperature, but provides the Ground Surface Temperature (GST) data directly from borehole temperatures. Thermal rock properties (conductivity, diffusivity and in deep boreholes also heat production rate) should be known, assumed, or determined as a part of the inversion process. Borehole depth constrains the time range of the GST history that can be extracted from temperature logs. Temperature profiles of 500 – 1 000 m depth cover approximately the last one–two millennia, whereas deeper holes are necessary to retrieve GST histories further back in time.

Inversion of GST history from borehole temperature logs has been extensively applied for paleoclimatic studies since the 1980's. Although the effect of paleo-temperatures on measured borehole temperatures has been known for a long time (e.g. Benfield 1939, Birch 1948). It took a long time until the particular value of extracting paleoclimate information from borehole data was recognized by

Čermák (1971), Beck (1982), Lachenbruch and Marshall (1986) and Lachenbruch et al. (1982). Heat flow data has been routinely corrected for climatic effects (e.g. Jessop 1971, Beck 1977, Kukkonen 1987). The utilization of subsurface temperature data as a source for paleo-temperature information emerged when inversion methods were taken into use in the problem. Numerous methods have been applied for GST inversions, but the most common ones are the singular value decomposition (SVD) method (Beltrami and Mareschal 1992, Beltrami et al. 1997), functional space inversion (Shen and Beck 1991), Monte Carlo inversion (Mareschal et al. 1999, Kukkonen and Jõeleht 2003), and numerical methods using different forms of deterministic Tikhonov regularization (Rath and Mottaghy 2007). In most of these methods, the model geometry is a 1D layered Earth. More complicated geometries have been modelled with forward methods (e.g. Kukkonen and Šafanda 1996). However, the typical lack of detailed spatial information on temperatures and thermal properties in the bedrock often prohibits a proper use of full 2D and 3D geometries. Also, the additional effort using 2D and 3D geometries seems only justified when there is a strong indication of lateral heterogeneity in bedrock properties. The state-of-the-art in the interpretation of borehole temperatures is presented in the reviews by González Rouco et al. (2009) and Bodri and Čermák (2007).

Sundberg et al. (2009) performed a paleoclimate and geothermal heat flow study using borehole temperature data from Forsmark. The present study constitute a follow-up to Sundberg et al. (2009), where we apply geothermal GST inversion methods on temperature and thermal property data from the Forsmark and Laxemar sites. In the SKB site investigation programmes performed at Forsmark and Laxemar, the usage of temperature data from deep boreholes has been limited to determining the temperature at the planned repository depth and to verifying water flow from hydraulic tests (SKB 2008, 2009). However, the temperature development towards depth contains more information that can be used to investigate (1) potential information on past climate changes that can be extracted from the temperature profiles; (2) the uncertainty associated with these paleoclimate reconstructions; (3) the climatological and environmental background to the temperature development at the drilling locations.

1.3 Previous work

In Sundberg et al. (2009), modelling of synthetic temperature and temperature gradient profiles were carried out for boreholes in Laxemar and Forsmark and fitted to measured borehole temperature data. The modelling was performed with an analytical expression including bedrock thermal conductivity, thermal diffusivity, heat flow, internal heat generation as well as a step-function describing estimated past air temperature variations.

One of the main objectives with the Sundberg et al. (2009) study was to calculate the paleoclimatically corrected surface mean geothermal heat flow for the two sites. Since there is no independent way to evaluate the heat flow, uncertainties in petrophysical data and the reconstructed paleoclimate ground surface temperature history (GSTH) are transferred into uncertainties in the heat flow.

Temperature data from a number of deep boreholes (typically down to 600–800 m) were available from each site. However, uncertainties in data, partly from thermal perturbation from drilling, made it impossible to select data from one single representative borehole from each site. For this reason, all temperature profiles from each site were merged to one single profile, judged to be the most representative for the site at hand and to satisfy the objective calculation of the paleoclimatically corrected surface mean geothermal heat flow. Since the analytical expression, used for calculation heat flow, did not allow for variable thermal conductivity and diffusivity along the boreholes, it was logical to use mean values for the petrophysical data in order to calculate the effective large scale heat flow values for each site. Separate calculations were made for the 1 700 m long borehole in Laxemar, KLX02. Note that while reducing the effect of heterogeneity in the physical properties, merging and averaging of temperature profiles does not eliminate the influence of perturbation due to drilling. As pointed out by Demezhko and Shchapov (2001) and Demezhko et al. (2013), the effect of an insufficiently restored regime in the simplest case is manifested in a decrease in the geothermal gradient and, therefore, in an overestimated paleotemperature prior to reconstruction, with an underestimated amplitude of the paleoclimate signal. Data quality on temperature logs are further discussed in Chapter 2.

The available proxy data reconstruction of GSTH for the Forsmark and Laxemar sites reach 120 kyr back in time (SKB 2006). From sensitivity analysis it was obvious that the temperature gradient was affected by paleoclimate temperatures more than 240 kyr back in time (i.e. longer than one glacial

cycle, which equals approximately 100 kyr), especially at larger depths. For the purposes in Sundberg et al. (2009), the long-term glacial cycle climate was assumed to be generally cyclical in nature. Therefore, the temperature models used in the modelling were extended to 228 kyr BP (Figure 1-1), where the ground surface temperature model reconstructed for the last glacial cycle was used also for the penultimate glacial cycle. A coarse reconstruction of the timing and conditions specifically for the Eemian interglacial, separating the last and the penultimate glacial cycle at around 130–120 kyr ago, was also made.

The surface mean heat flow, corrected for paleoclimate, at Forsmark and Laxemar was calculated to be 61 and 56 mW/m^2 respectively (Sundberg et al. 2009). If all uncertainties were combined, including the ones associated with the thermal data but excluding uncertainties in the given paleoclimate, the total uncertainty in the heat flow determination was judged to be within +12 % to –14 % for both sites. The corrections for paleoclimate are large (approx. 24–20 mW/m^2 respectively) and verify the need of site-specific climate descriptions.

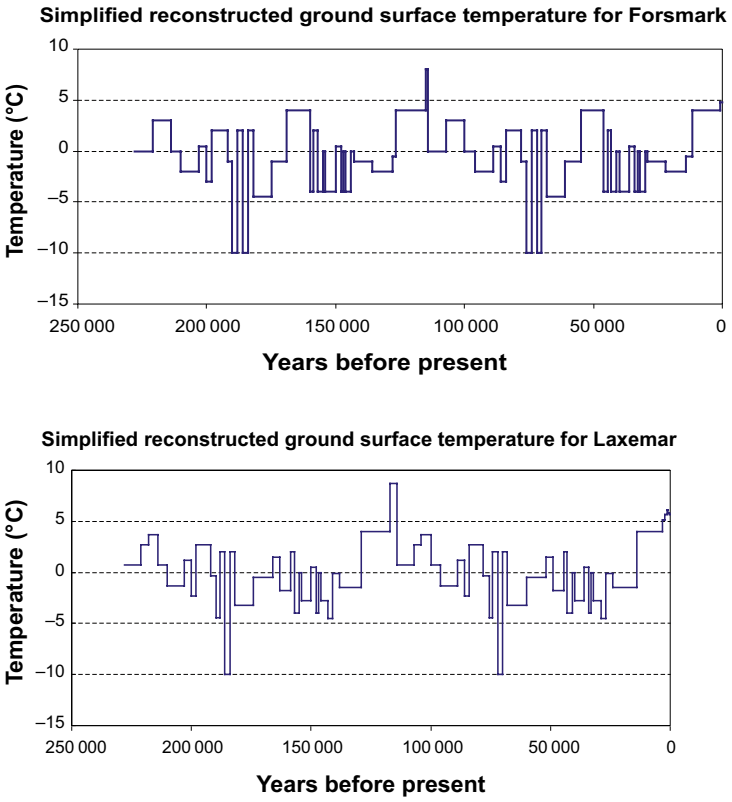

Figure 1-1. *Step model of ground surface temperature variations for Forsmark* (left) *and Laxemar (right), modified from SKB (2006). Note that temperatures during the last glacial cycle (the Weichselian), i.e. for the past ca. 120 kyr, have an uncertainty of several degrees. Temperatures during the penultimate glacial cycle (the Saalian glaciation) are estimated in a simplistic way by repeating the conditions reconstructed for the last glacial cycle, and should not be taken as representative of realistic conditions, see Sundberg et al. (2009).*

2 Description of the sites and borehole temperature data

The Forsmark area is located in northern Uppland within the municipality of Östhammar, east-central Sweden (Figure 2-1). It consists of a major tectonic lens formed between 1.87 and 1.85 billion years ago during the Svecokarelian orogeny. The boreholes in Forsmark were drilled into a metagranite, inside the tectonic lens, and dominated by rocks of granite and granodiorite composition (SKB 2008). The area is very well investigated and described in the site description presented in SKB (2008) and in underlying reports.

The Laxemar-Simpevarp area is located within the municipality of Oskarshamn, in the Småland province, southern Sweden (Figure 2-1). The site consists of a 1.8 billion year old suite of well-preserved bedrock belonging to the Transscandinavian Igneous Belt formed during the waning stages of the Svecokarelian orogeny. It consists of three rock domains with variable mineral composition both within and between the domains (SKB 2009).

Thermal data for the two sites is summarized in Table 2-1. Problems with data quality in the temperature loggings have been identified during the site investigations. Temperature logging data from boreholes with acceptable quality was put together to one representative log for each site. The quality criteria considered, discussed more fully in Back et al. (2007) and Sundberg et al. (2008b), were i) errors associated with logging probe and ii) time between drilling and logging. The resulting mean temperature profiles for Forsmark and Laxemar, used in the present study, can be seen in Figure 2-2. The temperatures measured in the deep KLX02, see Figure 2-6, in Laxemar (outside the site description area), were also used as base for separate inversions in the present study. However, acceptable data quality in the temperature loggings for the purpose of site description modelling does not necessarily mean that the data quality is good enough for the purpose in the present report. Remaining perturbation from drilling may have an influence in the inverse modelling and cause larger uncertainty.

Figure 2-1. *Location of the Forsmark and Laxemar sites.*

Table 2-1. Mean thermal data for Forsmark and Laxemar (Sundberg et al. 2008a, b, Back et al. 2007, Sundberg et al. 2009). The present-day mean air temperature at Forsmark is from Alexandersson and Eggertsson Karlström (2001).

Parameter	Forsmark	Laxemar
Borehole temperature logs Mean temperature at 2 m intervals	Based of temperature logs from 8 different boreholes	Based of temperature logs from 5 different boreholes
Thermal conductivity at room temperature	3.75 W/(m·K) Small variations for > 90 % of rock volume. Corrected for 4 % anisotropy in vertical direction.	2.75 W/(m·K) Large variation within and between rock domains. No correction for anisotropy.
Temp coefficient of Thermal conductivity	–10 %/100 °C	–3 %/100 °C
Heat capacity at room temperature	1.98 MJ/(m^3·K)	2.2 MJ/(m^3·K)
Temp coefficient of Heat capacity	+29 %/100 °C	+25 %/100 °C
Current air temperature	5.0 °C	6.4 °C
Current ground surface temperature. Extrapolated from borehole temperature logs	6.5 °C	7.3 °C (KLX02: 7.6 °C)
Heat production	2.7 µW/m^3	2 µW/m^3
Basal heat flow at 4 000 m	50 mW/m^2	48 mW/m^2 (KLX02: 46 mW/m^2)

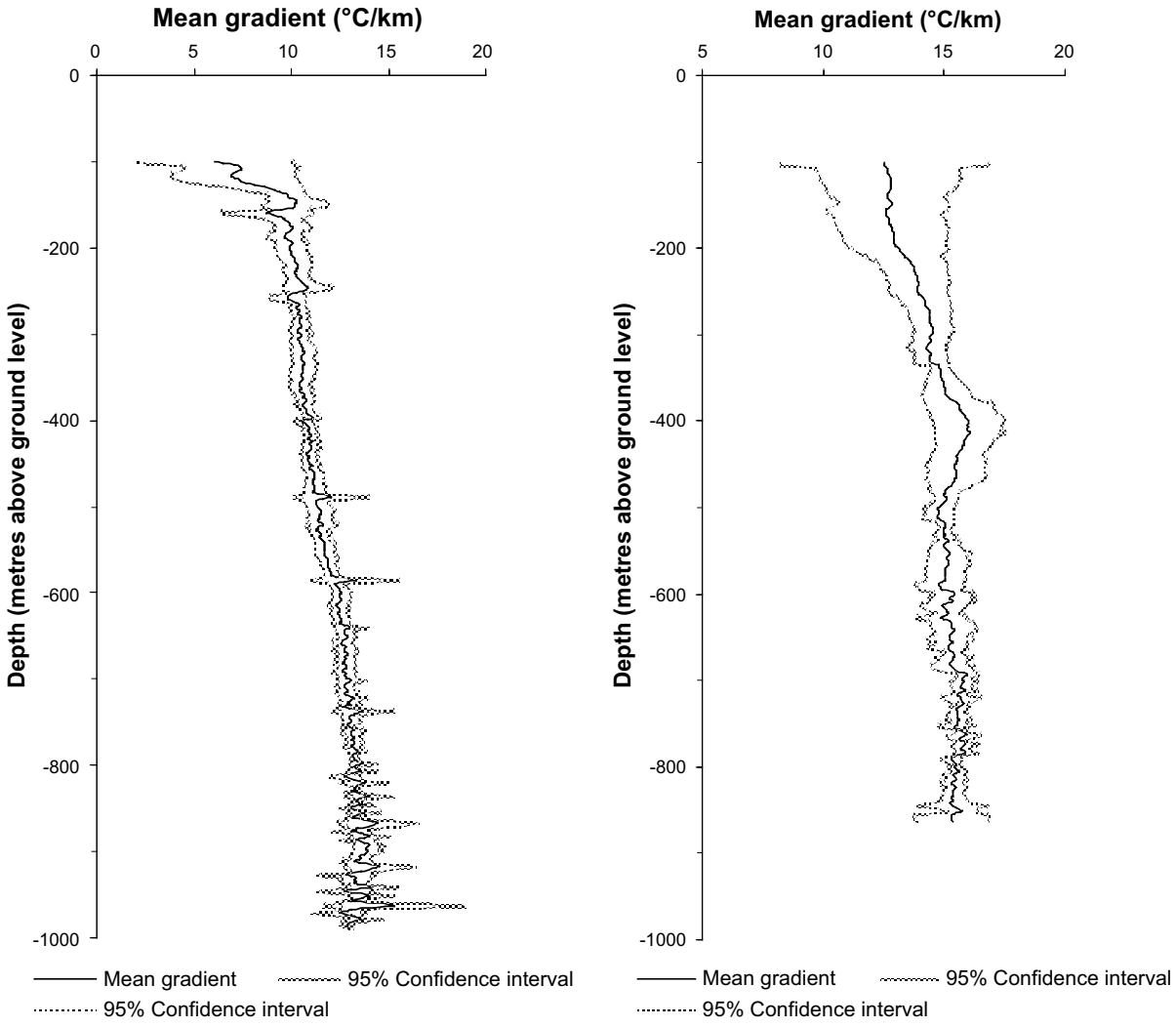

Figure 2-2. *Mean temperature gradient from the eight boreholes used from the Forsmark site (left) and the five boreholes used from the Laxemar site (right), from Sundberg et al. (2009).Measured temperatures and calculated gradients for all boreholes can be found in Sundberg et al. (2009).*

It is worth noting that the two study areas were deglaciated at different times. Laxemar-Simpevarp was deglaciated at ~14 kyr BP (~12000 BC) whereas the Forsmark area was deglaciated at ~10.8 kyr BP (~8800 BC), see Söderbäck (2008). Following the deglaciation, both sites were entirely submerged by water. The subsequent isostatic rebound gradually exposed the sites to terrestrial conditions, a process that still is ongoing today. Because of this gradual isostatic rebound, there are differences within each site when it comes to the timing of the transition to terrestrial conditions and the resulting duration of terrestrial conditions.

Table 2-2 shows the timing of the transition from marine to terrestrial conditions for the individual borehole locations in Forsmark and KLX02 in Laxemar, as well as the duration of terrestrial conditions up until the time of the temperature measurement in the boreholes. From Table 2-2 it is obvious that boreholes in Forsmark that are located at higher elevation, see also Figure 2-3, have experienced terrestrial conditions for longer periods of time than boreholes at lower elevations. In Table 2-2 and Figure 2-3 it can also be seen that the boreholes in Forsmark fall into two categories in terms of their duration of terrestrial conditions. Five of the borehole locations have been exposed to subaerial conditions for between c. 400 to 700 years, whereas three of them have been exposed for between c. 1 200–1 300 years. They have been grouped accordingly in Table 2-2. Since the boreholes in Forsmark can be grouped into two categories with different environmental- and thermal history, the temperature borehole data have also been averaged according to these two groups (Figure 2-3). This allows inversions to be made individually for the groups, for a discussion on the importance of local environmental histories.

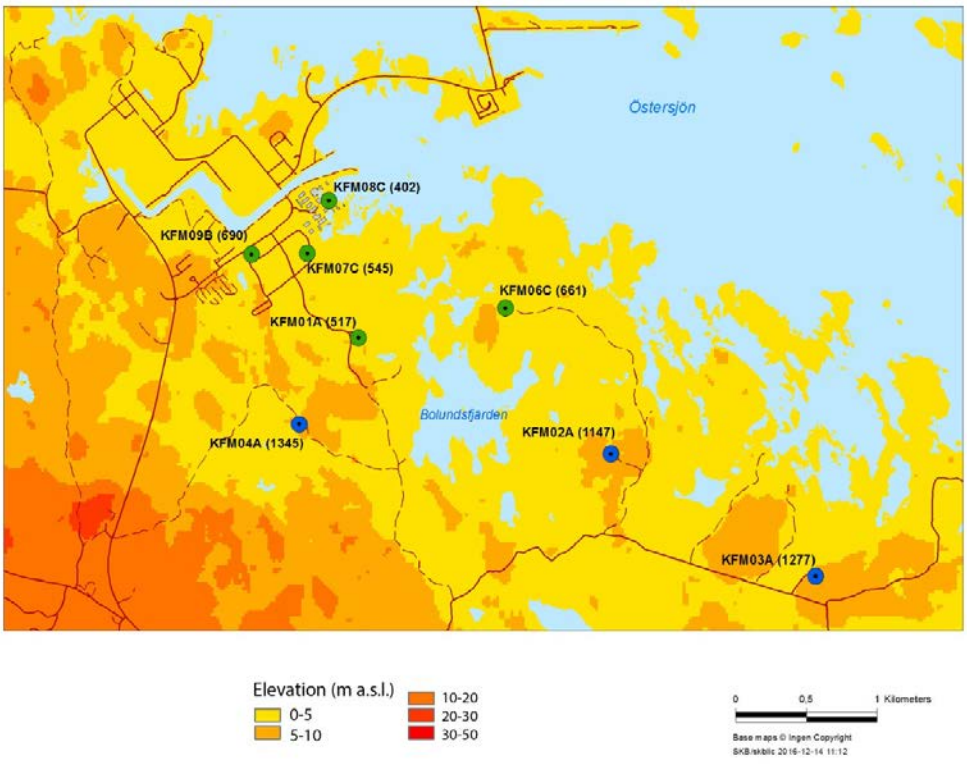

Figure 2-3. *Map showing the location of the eight bedrock boreholes (circles) included in this study at the Forsmark site (Figure 2-1). Numbers in brackets shows the duration of terrestrial conditions for the coring site expressed as years before temperature the measurements. Coring sites denoted with green circles have been exposed to subaerial conditions for c. 400–700 years, whereas coring sites denoted with blue colour have been subject to subaerial conditions for considerably longer time, c. 1 200–1 300 years (Table 2-2). The colours on the map represent elevation intervals according to the legend.*

Table 2-2. The boreholes used in this study and their respective i) elevation, ii) timing of transition from marine to terrestrial conditions following deglaciation of the sites, and iii) resulting duration of terrestrial conditions until the borehole temperature measurement. IDCODE = borehole ID, TOC = top of casing. Timing of terrestrial conditions is calculated according to Påsse (2001) and Hedenström and Risberg (2003). The Forsmark boreholes are grouped according to their duration of terrestrial conditions (group 1: approx. 400–700 years, group 2: approx. 1 200–1 300 years).

Site	Borehole IDCODE	Year of temperature measurement	Ground surface elevation	TOC elevation	Distance between TOC and ground	Timing of transition from marine to terrestrial conditions	Duration of terrestrial conditions until temperature measurement	Grouping of Forsmark boreholes according to duration of terrestrial conditions
			(m a.s.l.)	(m a.s.l.)	(m)	(BP, years before AD 1970)	(years)	
Forsmark	KFM01A	2003	3.04	3.12	0.08	484	517	1
Forsmark	KFM08C	2006	2.28	2.47	0.19	366	402	1
Forsmark	KFM07C	2006	3.20	3.35	0.15	509	545	1
Forsmark	KFM06C	2005	3.96	4.08	0.12	626	661	1
Forsmark	KFM09B	2006	4.15	4.30	0.15	654	690	1
Forsmark	KFM02A	2003	7.26	7.35	0.09	1 114	1 147	2
Forsmark	KFM03A	2003	8.17	8.26	0.09	1 244	1 277	2
Forsmark	KFM04A	2005	8.64	8.77	0.13	1 310	1 345	2
Laxemar	KLX02	2003	18.00	18.40	0.40	8 465	8 498	-

Separate inversions were made on one selected borehole from each group in Table 2-2, KFM01A (Group 1) and KFM02A (Group 2), in order to investigate if the difference in timing of the transition could be verified by inversion of borehole temperature data. The selected boreholes are rather deep, approximately (1 000 m), and the temperature loggings were made 6 and 5 months respectively after drilling, indicating less disturbance from drilling compared to measurements made in the other boreholes. Moreover, the same type of temperature probe (century 9042, evaluated as “reliable”) have been used in the two selected boreholes and the short distance in time between the two loggings increase the probability that the identical equipment was used. Further, the two boreholes are situated in the same rock type in the central part of the homogenous candidate area with expected small variation in thermal conductivity.

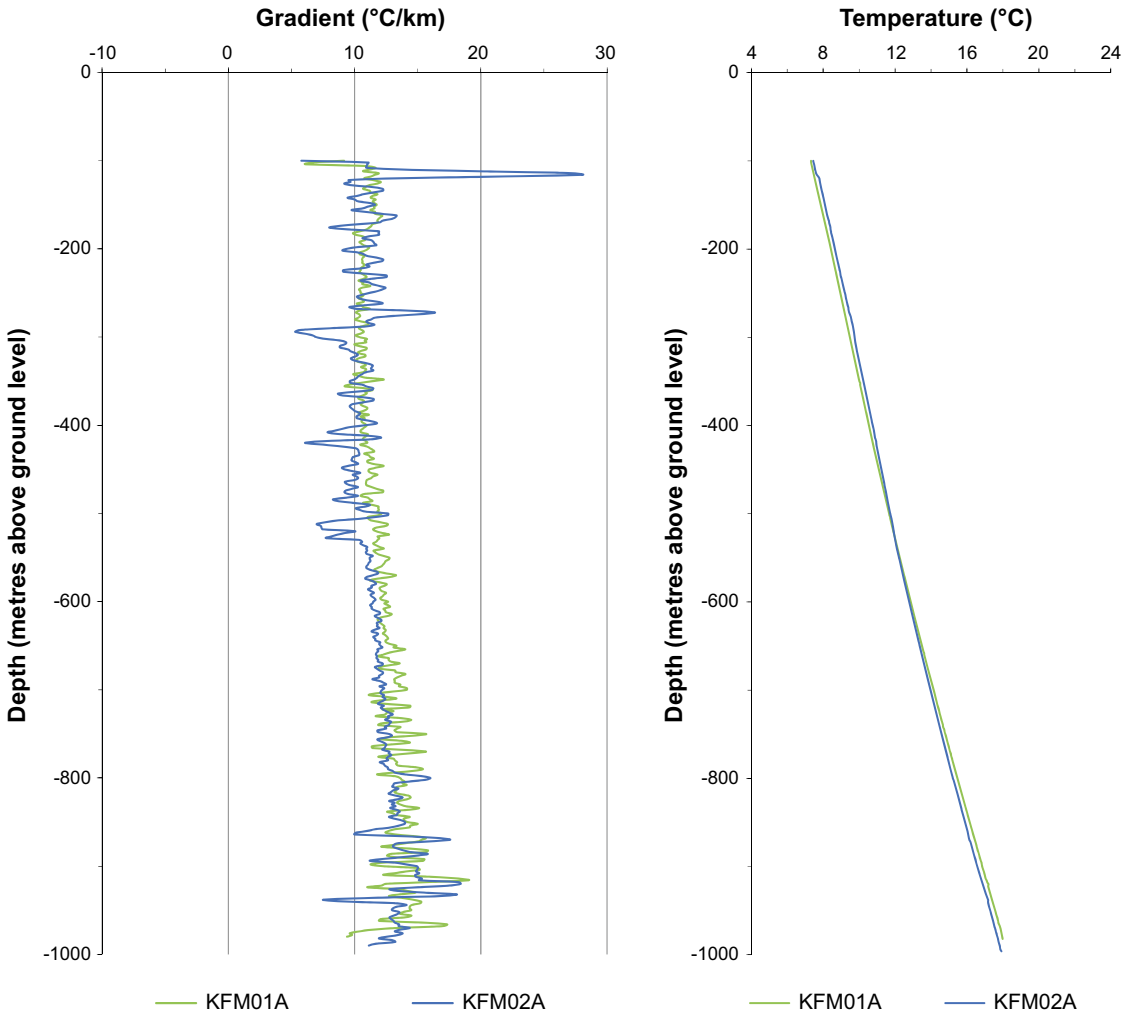

Figure 2-4. *Temperature gradients (left) and temperature (right) of KFM01A (green) and KFM02A. Green colours represent the borehole exposed for terrestrial conditions for the shortest time (group 1 in Table 2-2), whereas blue colours are exposed for the longest time (group 2 in Table 2-2). For locations of the boreholes, see Figure 2-3. Based on data in Sundberg et al. (2009).*

Figure 2-5 shows the location of the KLX02 borehole at Laxemar and Figure 2-6 shows the temperature gradient profile for the same borehole.

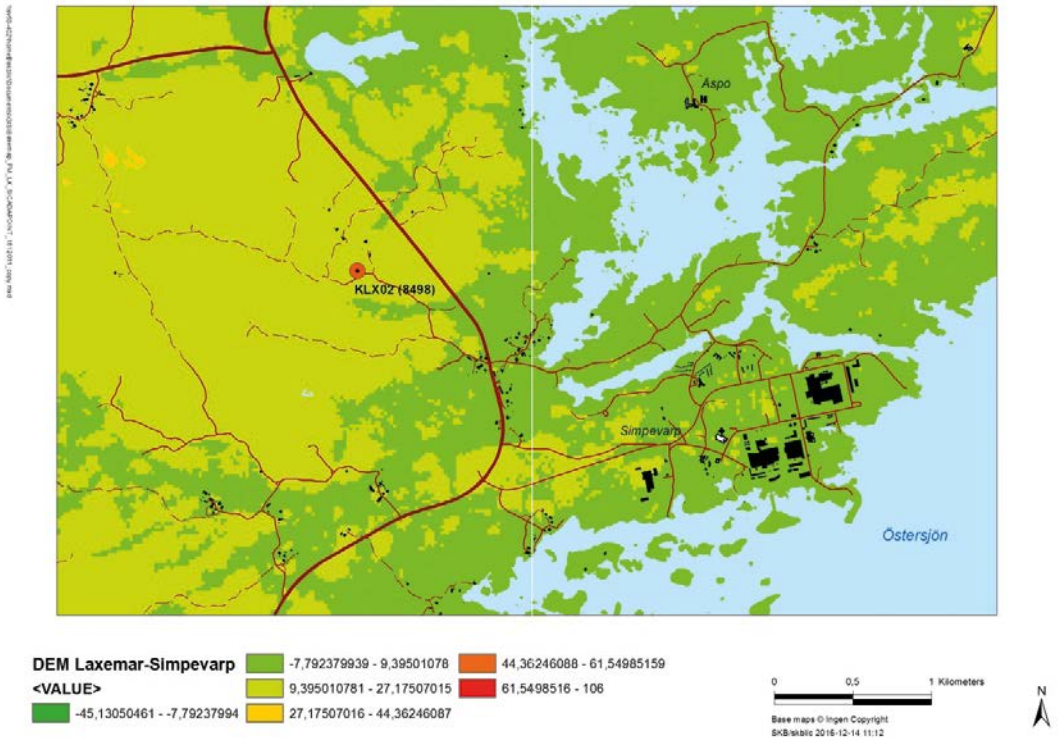

Figure 2-5. *Map showing the location of borehole KLX02 in the Laxemar-Simpevarp area (Figure 2-1). The number in brackets shows the duration of terrestrial conditions for the coring site expressed as years before the temperature measurement.*

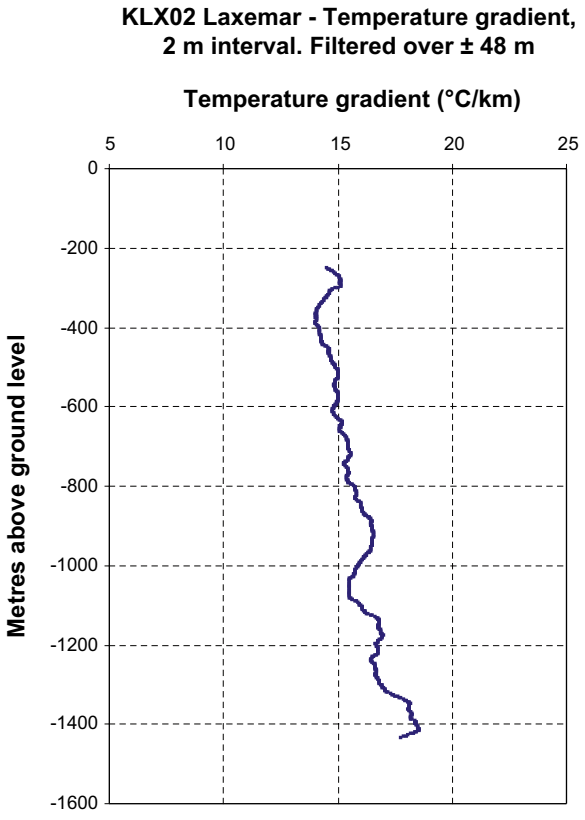

Figure 2-6. *The temperature gradient profile for borehole KLX02 (Sundberg et al. 2009).*

3 Physical and mathematical background

The approach described here was developed during the lead author's work on the Outokumpu scientific borehole (Kukkonen et al. 2011a, b) and Olkiluoto (Kukkonen et al. 2015), and were described in these publication. Here, we summarize the main elements for completeness.

The task of deriving meaningful estimates of past climate changes, in particular GSTHs, from recent borehole temperature profiles (BTP) is nontrivial, because the problem is strongly ill-posed in the nomenclature of Hadamard (1923). In a mathematical sense, the solutions to this problem may not exist, they may be non-unique, and possibly inherently instable. Hansen (1998, 2010) and Aster et al. (2013) give detailed accounts of this concept, and the techniques necessary to solve this kind of problems. In practice, this implies that the observed data (in this case the temperature measurements) need to be combined with knowledge from other sources to render the problem tractable. For the boreholes studied here, this additional information (as far as they are not introduced as explicit parameters in the Bayesian sense) includes a set of measured petrophysical properties, assumptions on the forward model used for the simulations, and on the general character of the solutions. It follows directly, that in these studies, the goodness-of-fit cannot be the single criterion for the quality of the solution.

Most current software for the estimation of GSTHs from borehole temperature profiles is based on a one-dimensional, conduction-only forward model. Thermal conduction in rocks is based on the theory given in Carslaw and Jeager (1959) for the heat conduction equation:

$$\left(\rho c\right)_e \frac{\partial T}{\partial t} + \frac{\partial}{\partial z}\left[\lambda_e \frac{\partial T}{\partial z}\right] - H = 0 \tag{3-1}$$

In this equation, H denotes the volumetric heat production (W/m^3), whereas the index e marks effective properties, i.e. properties which describe the rock-fluid two-phase system. As in the cases studied here porosity is very low, all properties will represent rock properties, and the e index will be omitted. The occurring physical parameters are the density ρ (kg/m^3) heat capacity cp (J/(kg·K)), and thermal conductivity λ (W/(m·K)), which in the case of spatially constant properties can be combined to define the diffusivity k (m^2/s) as:

$$\kappa = \frac{\lambda}{\rho c} \tag{3-2}$$

In order to solve Equation (3-1) we assume boundary condition of $T(z_0, t) = T_{GS}(t)$ at the surface, and

$$\frac{\partial T}{\partial z}(z_{\max}) = -\frac{Q_b}{\lambda_e} \tag{3-3}$$

at the base of the model domain. Q_b is the basal heat flow density at the base of the model, z_{max}.

The forward problem is solved by numerical finite difference techniques (e.g. Patankar 1980), allowing for a flexible discretization in both, time and space. As shown in Figure 3-1, temperatures in the forward finite difference (FD) modeling are associated to nodes, which mark the boundary of the cells. Thermal conductivity λ, density ρ, heat capacity c_p, and heat production H are associated with cells, but the latter is interpolated to the nodes for computational convenience. Time stepping is achieved by a Backward Euler or Crank-Nicholson scheme, which is complemented by possibly damped fixed point iteration for resolving the nonlinearities in the coefficients.

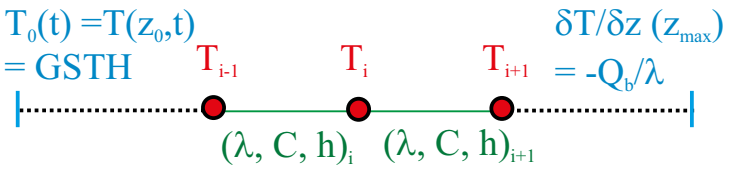

Figure 3-1. *Schematic description of the discretization used for the finite difference forward modeling. Measured data have to be assigned to computational nodes (red), while the properties are associated with the cells. Both may imply interpolations or averaging (upscaling) to a given grid for observed temperatures and measured petrophysical properties.*

4 Setup of the inversions

For the inversions presented here we used the deterministic approach presented in Rath and Mottaghy (2007), as well as a Bayesian stochastic approach with a Metropolis-Hastings Markov Chain Monte Carlo algorithm (Metropolis et al. 1953, Hastings 1970). Details of the techniques relevant to this report are given in Appendix 1.

4.1 General setup

For the FD model employed, the temperature data as well as the rock properties (thermal conductivity λ, density ρ, heat capacity c_p and diffusivity κ) measured in the laboratory are not known at the nodes or cell centers of the numerical FD model. Thus it is necessary to upscale or interpolate these point measurements to the nodes or cell centers, respectively. For the inversion models used here, we have used an equidistant grid down to the bottom of the BTP ($\Delta z = 4$ m), with a logarithmic increase for larger depths down to around 4 000 m.

In order to minimize boundary effects, the numerical mesh for the paleoclimate calculations has to extend to at least 4 000 m. At this depth basal heat flow density defined as:

$$\mathbf{q} = -\lambda \nabla T \approx -\lambda \frac{\partial T}{\partial z} \tag{4-1}$$

must be imposed as a Neumann (i.e. fixed gradient) boundary condition.

Below the depth of the borehole, the thermal rock properties were set to the averages for $z < 4\,000$ m, whereas the heat production term was set to zero. This guarantees that the HFD imposed at 4 000 m equals the one at 1 200 m, just below the depth of the borehole. The related errors in the approximation of the subsurface temperature field in the domain of the borehole are negligible. Unfortunately, the basal HFD has a decisive influence on the results of any paleoclimate inversion (e.g. Kukkonen et al. 2011a, b). In practice, it is determined by estimating the temperature gradient over an appropriate depth interval in the borehole, and the corresponding mean thermal conductivity. However, as demonstrated e.g. by Rath et al. (2012), the influence of the last glacial cycle leads to a downward bias in the top 2 000 m at least at mid- and high latitudes of the Northern Hemisphere. For the inverse modeling presented here, the basal heat flow density was thus included into the vector of estimated parameters for the Bayesian simulations, but not in the deterministic inversions.

Figure 4-1 shows the effect of the choice of the constant basal heat flow on a Tikhonov-type inversion as described in Appendix 1 (deterministic approach). In general we see that even though there are strong effects, the main effect is in the interval where the parameters are no longer well resolved. This leads to a dominance of the regularization term in Equation A1-1 in Appendix 1.

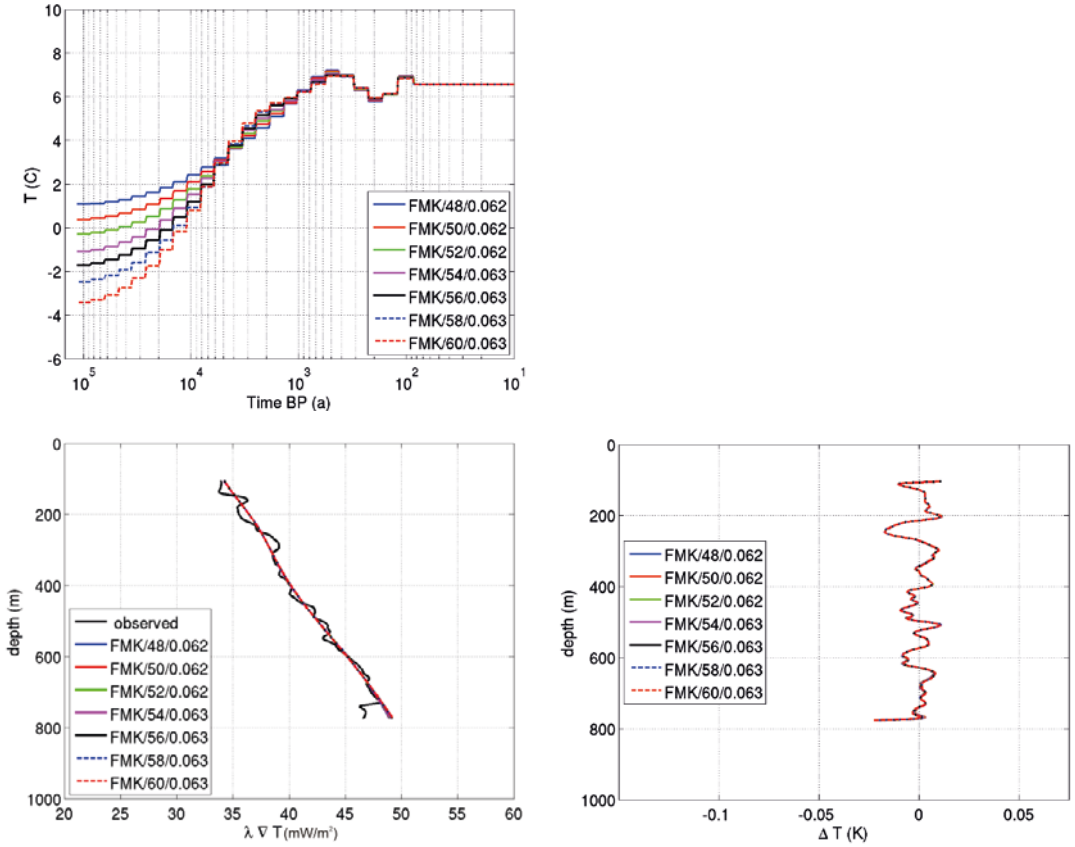

Figure 4-1. *Inversion results for Forsmark (deterministic approach) with different values assumed for the basal HFD, imposed at a depth of 4 000 m. The reconstructed GSTH for different numbers of step functions are shown in the top panel, while the corresponding residuals and heat flow densities are given below. These results were obtained with a regularization parameters $t_0 = 0$ and t_1 determined by GCV as defined in Equation (A1-7) in Appendix 1, leading to a divergence for times before 10 kyr BP. It is very clear that data carries only weak information on the basal heat flux, as they can be fitted equally well by values between 48 and 60 mW/m^2. This also implies that the uncertainty for the GSTH, for times before 4 kyr BP, is very large.*

Rock properties have been measured for the whole depth of the boreholes, giving, in principle, the possibility of a detailed profile. The BTPs, interpreted in this report, were constructed from average properties, assumed for the whole range of the borehole. Since porosity is generally very small (~1 %) it can be safely neglected. In addition, for numerical reasons the model has to extend to large depths in order to avoid undesirable effects of the boundary conditions. Thus, thermo-physical properties have to be assigned for domains which are not sampled by measurements, and temperature dependencies of the rock matrix were adopted. For this purpose, the values given in Posiva (2012) were fitted with a function given by Mottaghy et al. (2005) and Mottaghy (2007), which largely agree with the values given in Sundberg et al. (2008b). The effect on the paleoclimate inversions, however, is not very large and was neglected in subsequent simulations (see Figure 4-2). It has to be kept in mind that only rather small changes in temperature (< 10 K) are inverted for.

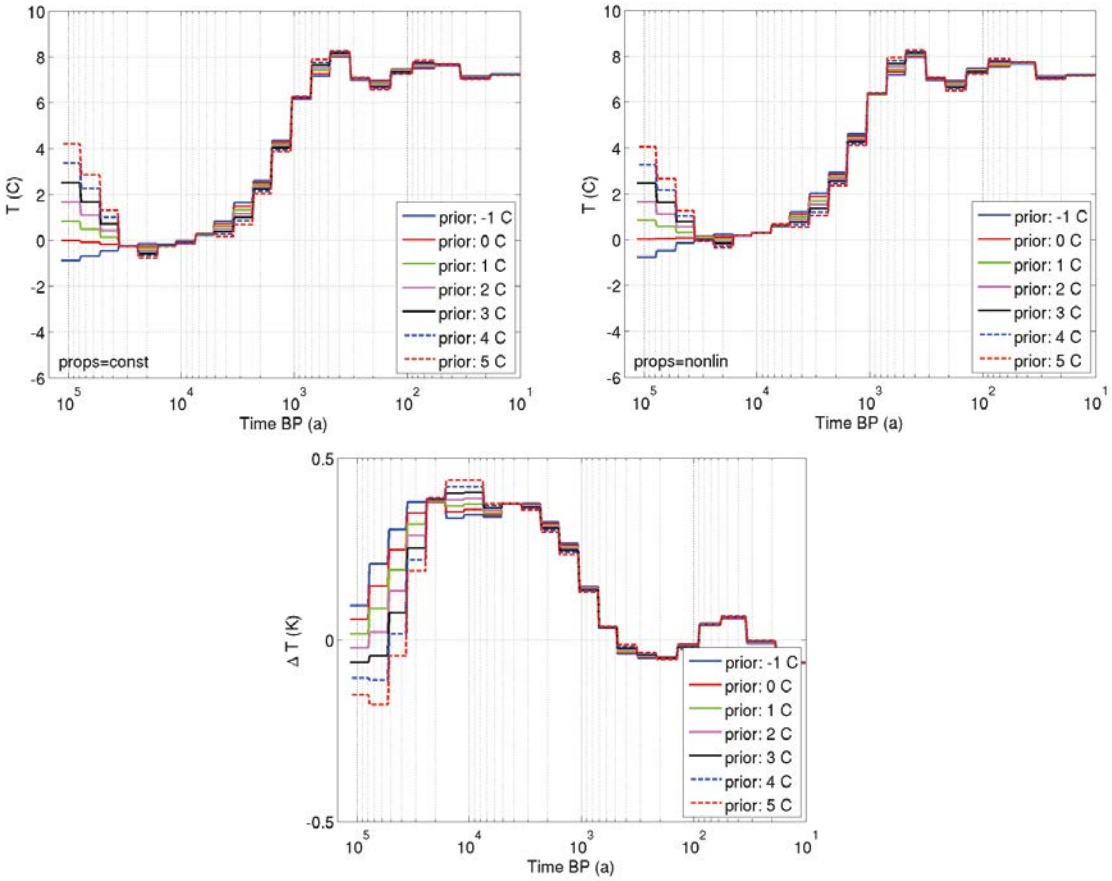

Figure 4-2. *Sensitivity of the obtained results to the nonlinear temperature dependencies of the coefficients $(rc)_e$ and l_e representing the effective properties in Equation (3-1). Top row: Inversion results assuming constant or temperature-dependent rock properties. The maximum effect is less than 0.5 K. The second row shows the effect of choosing different constant inversion priors.*

For the particular problem of borehole paleoclimate models which extend back to more than 120 kyr BP, a logarithmic time stepping is chosen, starting with very large steps (around 1 800 years at 120 kyr BP), which are reduced to very short steps near the present (reaching around one month at 10 years BP). This matches the physical character of the underlying conductive process, which reduces the high-frequency content of the GSTH with increasing depth, see Mottaghy and Rath (2006) and Rath and Mottaghy (2007). All inverted GSTHs are referenced to the year 2000 AD. For both sites, Forsmark and Laxemar, we used the same parametrisation for the GSTH with 25 piecewise constant intervals distributed logarithmically on the time axis, with increasing lengths backward in time, (Figure 4-3). This choice represents a trade of between the desirable resolution, and the computational effort. This is particularly important when using a stochastic approach as the Bayesian simulations where the "curse of dimensionality" (Bellman 1961) rules. A simple numerical exercise using the deterministic approach described in the last section underpins that this approach leads to reasonable results.

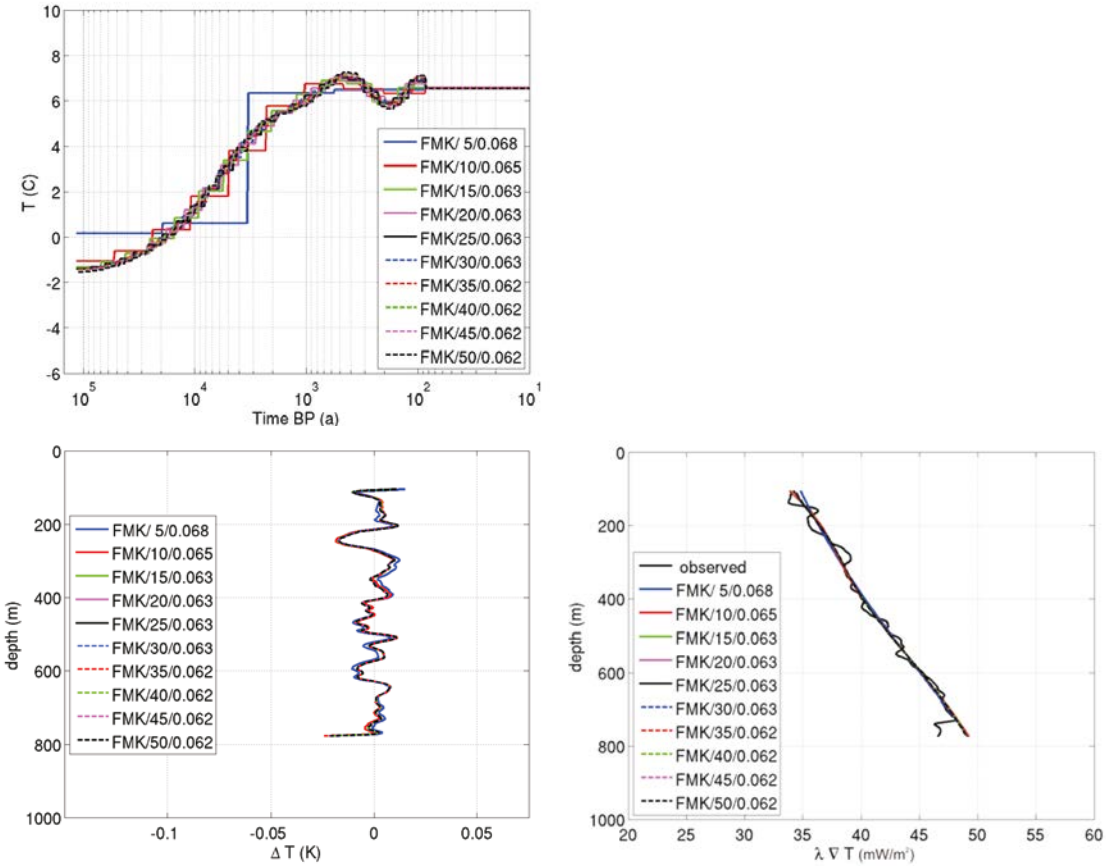

Figure 4-3. *Inversion results for Forsmark with different number of parameters, i.e. intervals of piecewise constant temperature. The two numbers in the legend mean the number of steps (parameters) and the corresponding RMS defined in Equation (A1-8) in Appendix 1. For these inversions, the regularisation is achieved using zero and first order terms as defined in Equation (A1-3). While t_0 is kept constant at a small value (0.003), t_1 is determined by GCV by Equation (A1-7). The reconstructed GSTH for different numbers of step functions are shown in the top panel, while the corresponding residuals and heat flow densities are given below.*

Finally, for the numerical solution of the forward problem, an initial condition is required. Here we have employed the following procedure. The forward model used for the inversion starts at 125 kyr BP. However, at this time the subsurface temperature cannot be assumed to be in thermal equilibrium, as glacial cycles have existed for a long time, and should in principle be part of the time-dependent model simulation. We tried to find a trade-off between computational resources and accuracy by constructing an approximate state of the system, which could be used as an initial value for the simulation. For this purpose we used the last glacial cycle temperature reconstruction presented in SKB (2006), adopting the simplification described in Sundberg et al. (2009) as forcing for our 1D simulations (Figure 4-4).

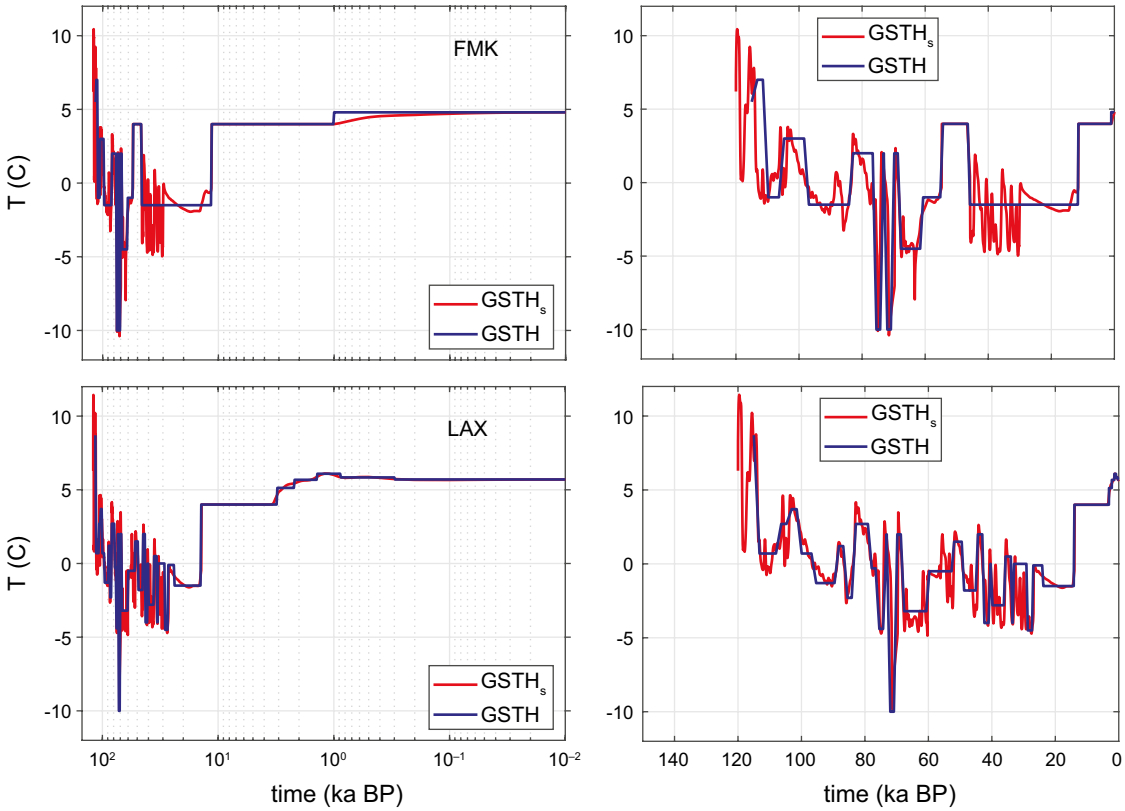

Figure 4-4. *GSTH forcings for Forsmark (top) and Laxemar (bottom) based on SKB (2006) and Sundberg et al. (2009). Note that on the left we present the GSTH on a logarithmic scale, as this corresponds approximately to the "weights" of the parameters in the inverse modelling. For the construction of the initial values of the paleoclimate models these patterns were used.*

Using these forcings, forward models were run iteratively for several (up to 10) cycles, taking the output of the last iteration as initial value for the current. The converged result was stored and subsequently used as initial state for the inversion runs. As an example, the initial temperature profile for Laxemar is shown together with the corresponding equilibrium in Figure 4-5.

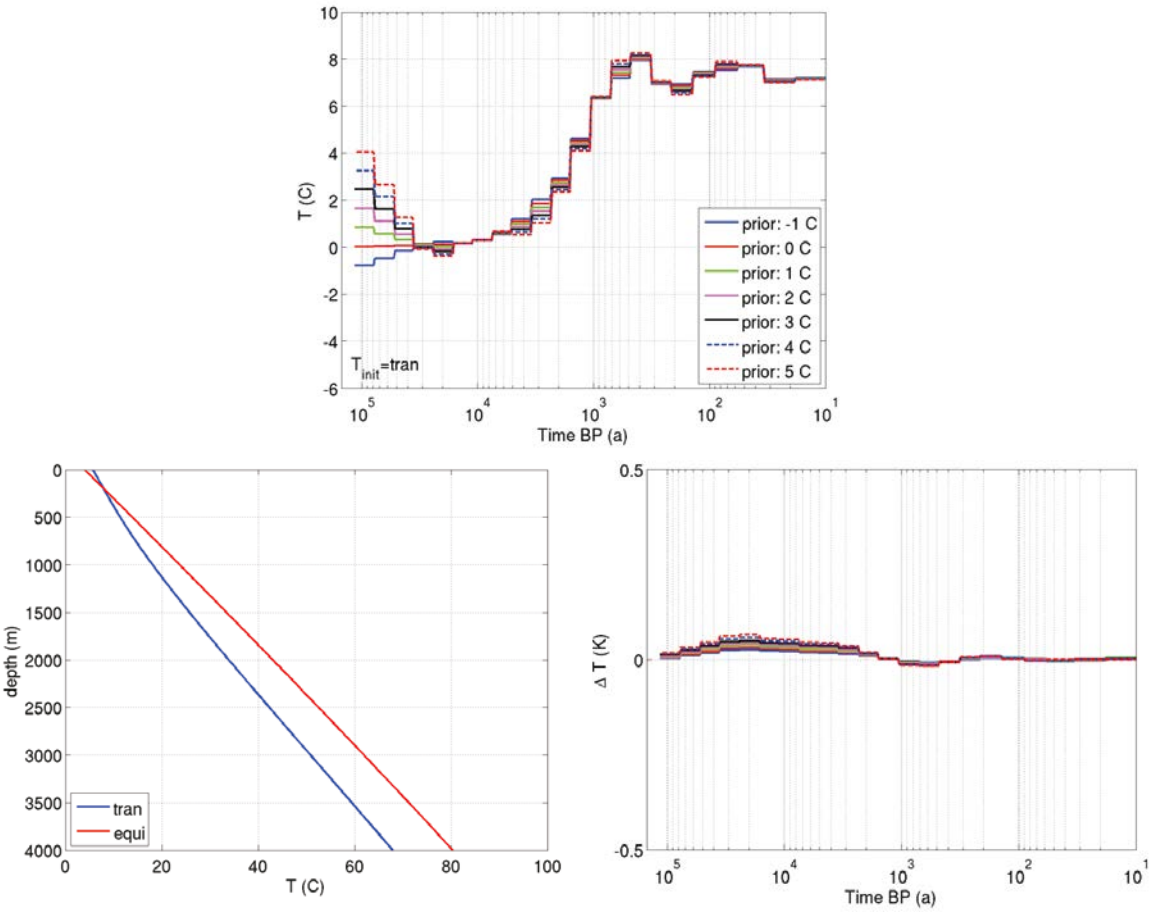

Figure 4-5. *Sensitivity of the obtained results to the chosen prior values for the GSTH and the initial conditions for Laxemar and based on SKB (2006) and Sundberg et al. (2009). Top: Inversion results for values of the constant prior model between –1 °C and 5 °C. The priors mainly affect the early times, where no information is present in the borehole profile. Bottom left: Initial temperatures for the Laxemar site. The red curve is the equilibrium (steady-state) distribution based on the modern surface temperature, while the blue one was calculated by the iterative procedure described in the text. Bottom right: difference in inversion results for both initial values value. The effect is generally below 0.1 K.*

4.2 Forsmark setup

As Sundberg et al. (2009) pointed out, there is no single deep borehole temperature profile which fulfils the requirements for a high-quality paleoclimate inversion. Therefore, we have the BTP constructed in a similar manner as described in Sundberg et al. (2009). This means that the data used for the inversion are averaged from eight boreholes scattered over an area of considerable extent (Figure 2-3) but with low variability in thermal properties. In addition, selected data from the boreholes that were grouped according to similar environmental history (Figure 2-4) were also used for a simplistic inversion test to study the impact of the duration of terrestrial conditions at the drillsites (Section 5.1.2). Due to significant noise in the top 100 m, this part of the log was disregarded, implying that there is no recoverable information on the GSTH for the last 100 years. At depths larger than 750 m, the differences in length between the boreholes lead to artefacts which made it inadvisable to use this interval. The computational grid was uniform down to 1 000 m with a Δz of 4 m, and the "measured" temperature profile was interpolated correspondingly to the nodal values, using linear interpolation with a following 3-point triangular smoothing operation.

In Figure 4-6 we show the sensitivities of the BTP data with respect to the paleo-temperatures for the model described in this section. These sensitivities, defined as the rows in the Jacobian matrix J which correspond to the piecewise constant intervals centred at 8, 2.2, 0.59, and 0.16 kyr BP. It is easy to see that we cannot expect resolution for very recent times (less than 100 years BP), or beyond the Holocene (approximately the last 10 kyr). This is due to the missing top 100 m in the data, and the short temperature log of less than 800 m. Likewise, it should be noted that because of the diffusive nature of the underlying physical process, the sensitivity with respect to the older surface temperatures cover a wide interval of the observations.

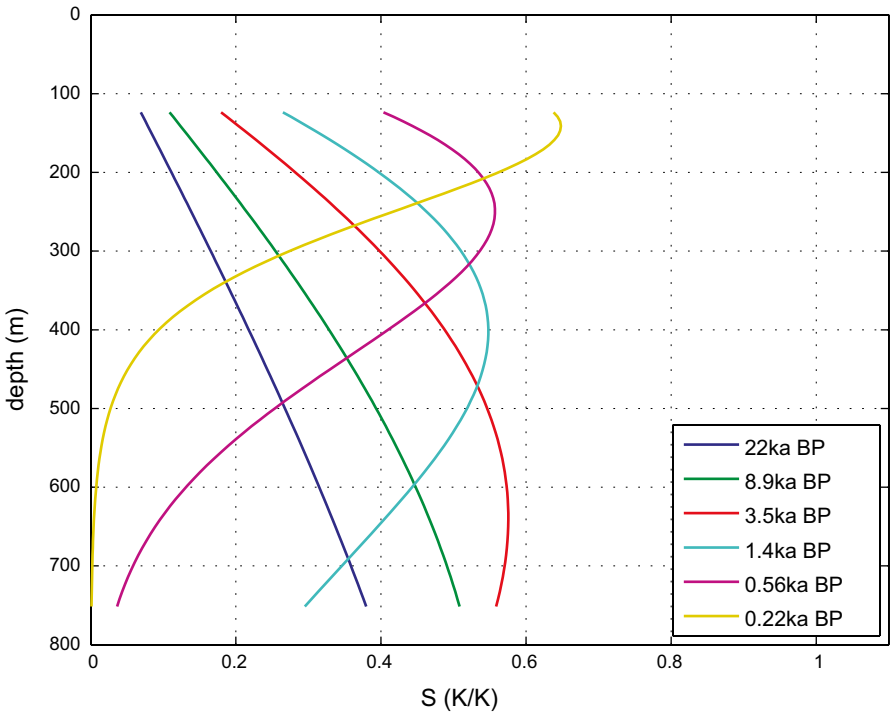

Figure 4-6. *Sensitivity of borehole temperatures with respect to four time intervals in the past, results for the Forsmark borehole. It can be seen that we cannot expect resolution for very recent times (less than 100 years BP), or prior to the Holocene (approximately the last 10 kyr). As the sensitivity is the partial derivative of a temperature (measured in the borehole) with respect to a temperature (step in the GSTH), it has the dimension of K/K.*

The parameter settings for Forsmark can be found in Table 4-1. These properties were used down to the full depth of the numerical grid (4 000 m). For the MCMC (Markov Chain Monte Carlo technique) simulation we used a prior parameter vector $\boldsymbol{m}_a$ which comprises a GSTH of 25 piecewise constant intervals, covering the time interval between the present and 120 kyr BP. This GSTH was initialized to a constant value of +5 °C, which was slightly perturbed randomly for each independent chain. As numerical experiments had shown a significant relationship between the early GSTH parameters, and the assumed basal heat flow density Q_b this parameter was included as well. In the case of Forsmark, it was initialized to 55 mWm^{-2}. The values of the standard deviations corresponding to these means of the initial prior distribution were 2.5 K and 3 mWm^{-2}, respectively. The correlation length L in Equation (A1-10) was set to 5. The approximate volumetric heat production H was taken from Sundberg et al. (2009).

Table 4-1. Parameter settings used as prior in the MCMC calculations for the Forsmark borehole. After numerical tests concerning the role of the radiogenic heat production, this parameter was also held fixed for the simulations. The values assumed here were motivated by the studies by Sundberg et al. (2009). Within the Bayesian approach, the posterior distributions of the included parameters (GSTH and basal heat flow density) will deviate from the priors.

Parameter	λ	$\rho\, c_p$	H	Q_b
SI unit	($Wm^{-1}K^{-1}$)	(MJ/m^3K)	($\mu W/m^3$)	(mW/m^2)
$\mathbf{m_a}$	3.5	1.98	2.3	55
$\boldsymbol{\sigma_a}$	-	-	(0.5)	3

4.3 Laxemar setup

In the Laxemar area, we used the data from the Laxemar compound log (Figure 2-2), but also the deeper temperature log at borehole KLX02, see Figure 2-6, as described in Sundberg et al. (2009). The Laxemar and KLX02 inversions were run with constant thermal properties, which were taken from Sundberg et al. (2009). As in the case of Forsmark, we kept the mesh uniform down to about the maximal depth of the observations of 900 m and 1 500 m, respectively, with a Δz of 4 m. The "measured" temperature profile was interpolated correspondingly to the nodal values using linear interpolation, and a 3-point triangular smoothing operation.

Table 4-2. Prior parameter settings used for the MCMC calculations for the Laxemar and KLX02 boreholes..For the simulations the petrophyical parameter were held fixed, while the volumetric heat production and the basal heat flow density were included in the inversion. The resulting posteriors will not depend on the choice of the priors for these parameters.

Parameter	λ	$\rho\, c_p$	H	Q_b
SI unit	($Wm^{-1}K^{-1}$)	(MJ/m^3K)	($\mu W/m^3$)	(mWm^2)
$\mathbf{m_a}$	2.7	2.16	2	45
$\boldsymbol{\sigma_a}$	-	-	(0.5)	3.5

5 Results

5.1 Forsmark

5.1.1 Results using the averaged compound temperature data

The results from the MCMC simulations using the averaged compound temperature data (Figure 2-2) are shown in Figure 5-1 to Figure 5-3. In the following, we summarize the important observations concerning these results.

The data fit for Forsmark is excellent. For the full length of the temperature log, the residual is less than 0.025 K, a level only rarely reached in this kind of inversion. The reason for this is probably that the assumption of a constant average with high-frequency perturbations is valid for this log. The additional smoothing applied during the processing lead to a reasonably accurate representation of the true conditions.

The interval of reconstructed surface temperatures which can be trusted is approximately between 30 yr BP and less than 10 kyr BP. For this reason it is not clear, whether the decrease in temperature in the last 30 years is real or an artefact of the prior value assumed. In the case of the very recent period, it has to be kept in mind the top 100 m of the temperature measurements had to be neglected. At times prior to 10 kyr BP, the estimated GSTH show considerable scatter Figure 5-1, visible as a large spread of the solutions in both the global distribution and the median results from the single chains. The scattered results for the times before 10 kyr BP should not be taken too seriously, as the sensitivity of the data is very low for these time intervals. This applies in particular to the temperature decrease during the last glacial cycle. The scatter is also strongly related to the rather wide distribution obtained for the basal heat flow density (Figure 5-3).

Within the reliable interval, we find a rather clear signature of the little ice age (LIA) between 100 and 300 years BP. The medieval warm period is less clear. The most striking feature is the abrupt rise in temperature near 1 500 years BP. The amplitude is about 3 K, and starts from a level of about +4 °C. Again, this feature is present in all independent chains. This gives us an indication that this is a feature necessary to explain the data. Basal HFD, which is one of the additional outputs of the MCMC simulations, follows a rather wide distribution centred at the median of 52.6 and 68 % quantiles of 51.3 and 54.0 mWm^{-2}. It displays a small skewness to higher values. The corresponding mean value and standard deviation would be 53 ± 3 mWm^{-2}.

The covariance adaption scheme proposed by Haario et al. (2006) worked well. This is corroborated by the high grade of similarity of the independent MCMC runs. The GSTH obtained by these simulations also agree well with the ones from the deterministic (Tikhonov) schemes, which however display more smoothing as a result of the strong regularization employed here. A summary of the GSTH obtained by both methods is given in Figure 5-4.

5.1.2 Results using temperature data from boreholes with known different environmental histories

Figure 2-3 shows the borehole temperatures in Forsmark grouped according to environmental history. The boreholes in group 1 have a shorter period of marine conditions and a longer period of terrestrial conditions during the Holocene compared to the boreholes in group 2. The borehole/temperature log judged to be of best quality in each group was selected for a simplistic inversion calculation (KFM01A from group 1 and KFM02A from group 2, see Figure 2-4). The results of this inversion (using two different model settings) are seen in Figure 5-5. Even though the model parameters are not optimized in these simulations, a tentative interpretation of the results is that FMK02A shows a 1.5–2 degree temperature increase at around 1100 BP (around the medieval climate optimum). This climate signal is absent in FMK01A, see the discussion.

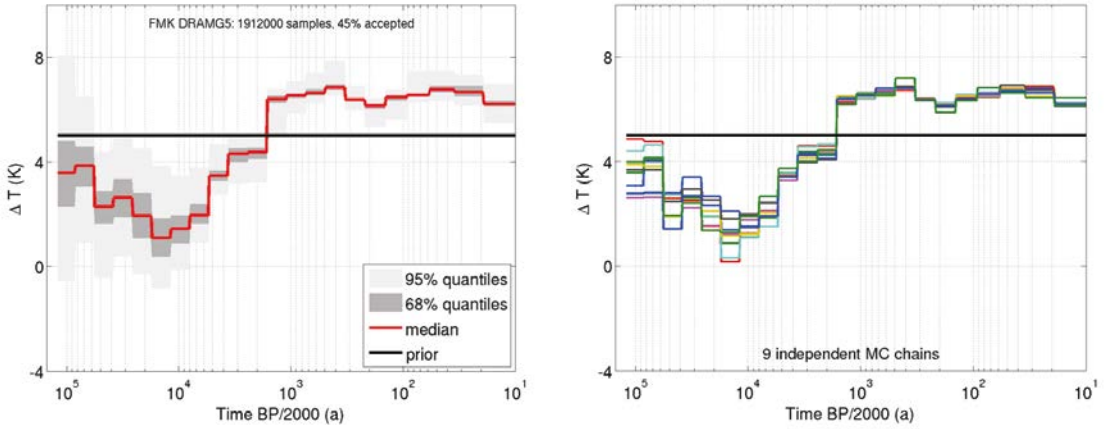

Figure 5-1. *Results from the Bayesian (MCMC) simulation for the Forsmark mean composite temperature log. It is based on an ensemble of $N \approx 2 \times 10^6$ samples. Left: Density plot of GST history. The shading defines the 68 % and 95 % quantiles. The median of the ensemble is shown in red, together with the prior (black). Right: Results from nine independent MC chains, each of about 200 k samples. The constant prior model (+5 °C) is marked in black.*

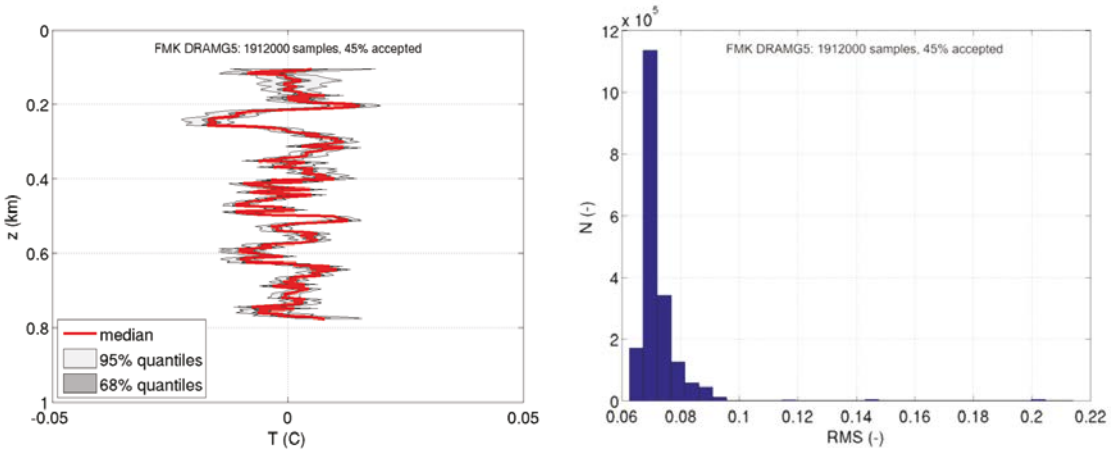

Figure 5-2. *Left: Residuals for the ensemble. Right: RMS corresponding to the ensemble.*

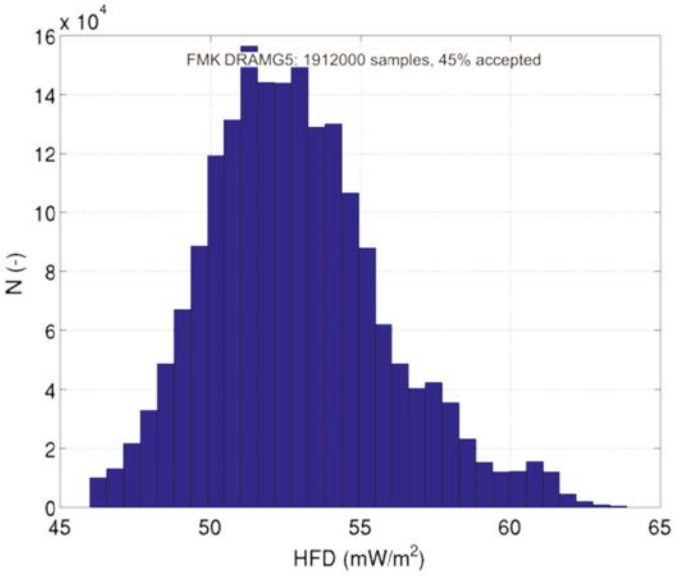

Figure 5-3. *Results for the HFD estimation from the Bayesian (MCMC) simulation for the Forsmark temperature log. The distribution appears slightly asymmetric with a bias to higher values. The median is 53 mWm^{-2}, with 68 % quantile values of 51.3 and 54.0 mWm^{-2}.*

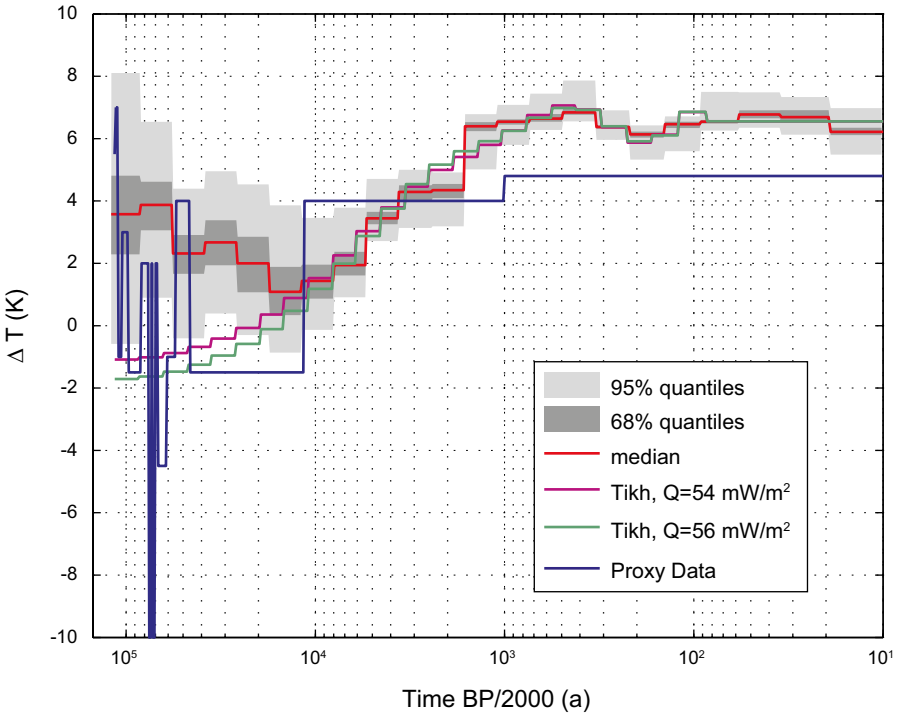

Figure 5-4. *Summary of GSTH inversion results for Forsmark. The inversions from both methodologies agree well back to several kyr BP. For times before the early Holocene temperature rise, the stochastic MCMC simulation (median) leads to comparatively warm conditions, whereas the deterministic inversions (Tikhonov) agree much better with the proxy data paleoclimate reconstruction (Proxy data)) used in Sundberg et al. (2009). This, however, is probably an effect of the strong regularization inherent to this method.*

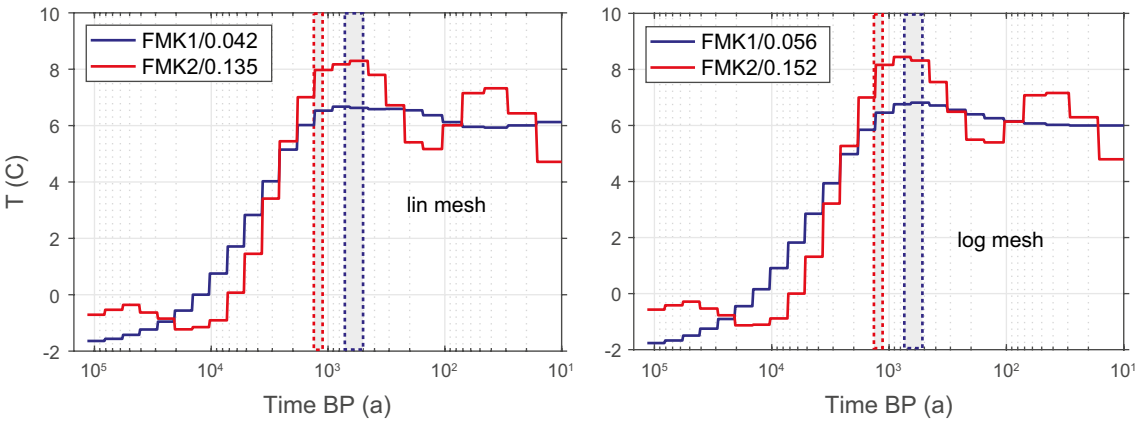

Figure 5-5. *Results of the inversions for the two boreholes KFM02A and KFM01A, with different Holocene environmental histories (KFM01A from group 2 with a longer terrestrial history and KFM02A from group 1 with a shorter terrestrial history, see Table 2-2). The left and right plots have different inversion model settings. The difference between the two is the spatial discretization, which is linear (left) and logarithmic (right). The discretization determines the distribution of data (temperature) values on the vertical axis. The logarithmic increase makes the sampling coarser for most of the borehole's depth. A tentative interpretation of the results is that FMK02A shows a 1.5–2 degree temperature increase starting at around 1100 BP, i.e. around the medieval climate warming period, absent in FMK01A (see discussion).*

5.2 Laxemar

The data fits for the Laxemar and KLX02 temperature profiles are in general considerably poorer than in the case of Forsmark. Furthermore, the corresponding residuals in Figure 5-6 and Figure 5-7 show much stronger systematic correlations, which indicate, that the underlying averaged properties do not well represent nature. These structured residuals probably are the main reason for the generally problematic results. This can be nicely seen in Figure 5-6 which shows conventional deterministic Tikhonov-type inversions for both boreholes. In particular the gradients show that the algorithm tries to adapt to the large deviations which probably correspond to heterogeneities of thermal properties at or near the boreholes which cannot be represented in the averaged properties. For this reason, we have concentrated on the results from the KLX02 simulations in this study.

We performed stochastic MCMC simulations in the same manner as was done for Forsmark for both data sets from the Laxemar area, with the a prior GSTH of constant 4 ± 2.5 °C for the full period, corresponding to an average value over the period of interest as determined from the earlier results from deterministic Tikhonov inversions. The prior standard deviation gives a variability which covers most of the probable conditions, and is adapted later in the MCMC process (Haario et al. 2006). The other priors were chosen as given in Table 4-2.

It was possible to derive a meaningful posterior GSTH with MCMC approach for KLX02 only, while the uncertainties for the Laxemar compound inversions remained unsatisfactory large and are not included in this study. KLX02 obtained a median RMS near 0.27, with the value for the Laxemar compound more than twice as large. This is about five times more than for the Forsmark case. The results from KLX02 simulations are shown in Figure 5-7.

In order to improve the results, we added the constant value of radiogenic heat production to the set of parameters included in the MCMC runs. As was expected from the numerical experiments shown in Figure 4-2, the data are compatible with a broad range of values for H, some influence was visible, with a posterior median value for the KLX02 log of about 1.4 $\mu W/m^3$, with 68 % quantiles of 1.1 and 1.6 $\mu W/m^3$. For the KLX02 simulation, we obtained basal heat flow values of 47.3 mW/m^2, with corresponding 68 % quantiles of 46.6 and 48.0 mW/m^2, respectively (see Figure 5-7, bottom).

With respect to the paleoclimate to be inferred, the results are quite similar to the ones in Forsmark during the last millennium. The development during earlier parts of the Holocene is quite different. Though the most prominent change in surface temperature occurs at the same time (1.5–2.5 kyr BP), the KLX02 GSTH reaches much lower temperatures, coming near the freezing temperature in the very early Holocene. It must be noted, however, that the data do not really resolve this time period, as the spread becomes large here, and the influence of the prior model increases.

Numerical experiments on KLX02 with deterministic inversion schemes (not included in this report), which employ stronger constraints, e.g. the W_1 or W_2 smoothness-enforcing operators as defined in A1-3 lead to similar but less detailed GSTH curves as the stochastic ones, irrespective of the particular type of regularization and number of parameters. However, the results presented here do not agree well with the paleoclimate reconstruction used in Sundberg et al. (2009), see Figure 5-8.

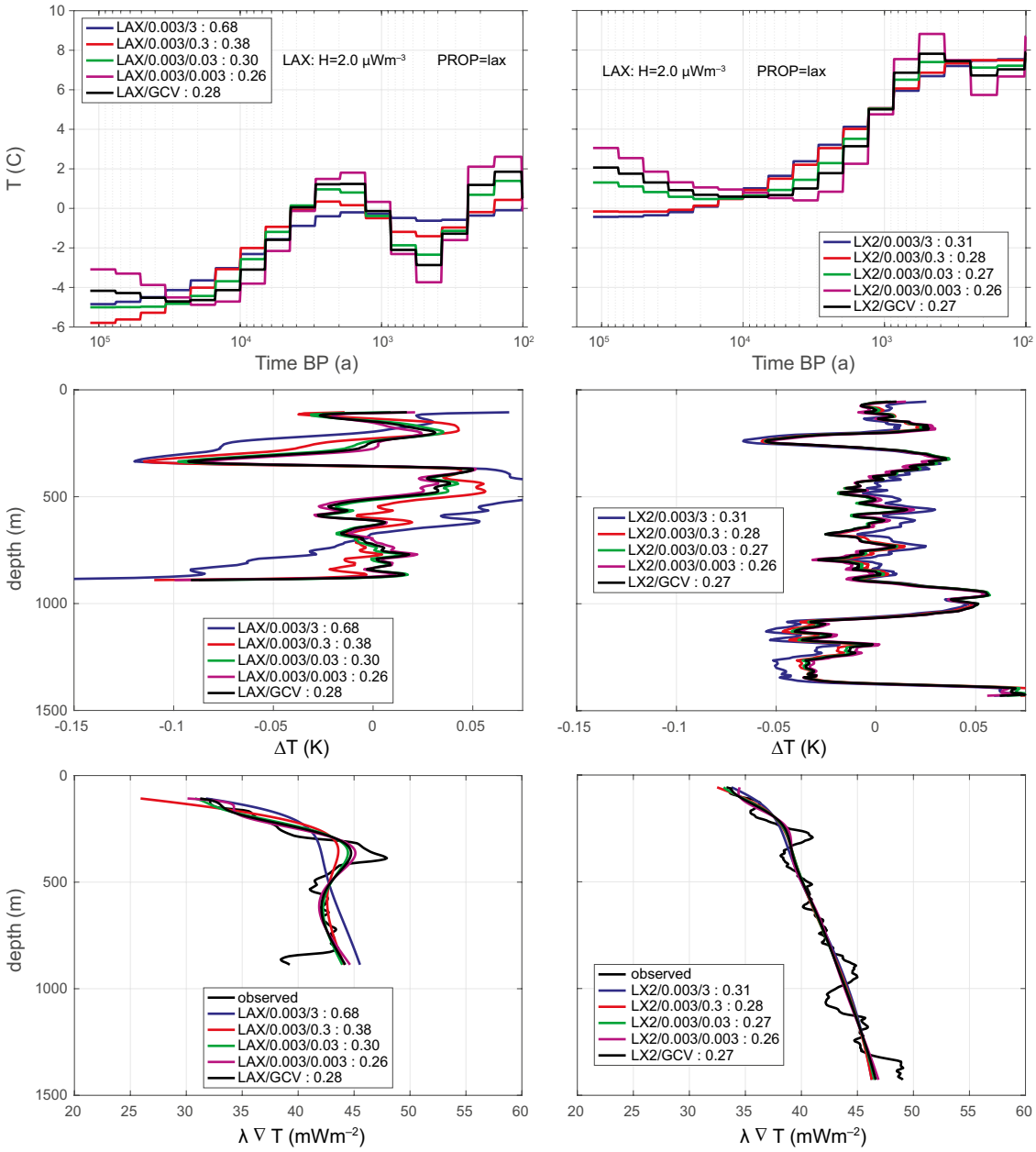

Figure 5-6. *Tikhonov inversions (deterministic approach) for the Laxemar compound (left), and KLX02 (right) temperature logs. In each panel results are shown for different choices of the regularization parameter τ_1, and an automatic determination by minimal GCV. Top: Estimated GSTH. Centre: Temperature Residuals; Bottom: Heat flows. These heat flows show nicely that the algorithm tries to adapt to the large deviations which may correspond to heterogeneities of thermal properties at or near the boreholes. The GST history estimated from Laxemar (LAX) must be considered highly improbable given the spatial relationship between both data sets. The simulations for this numerical experiments were run with the laboratory-derived average value of heat production H (2 mWm^{-3}) and a basal heat flux density of 47.0 mW/m^2.*

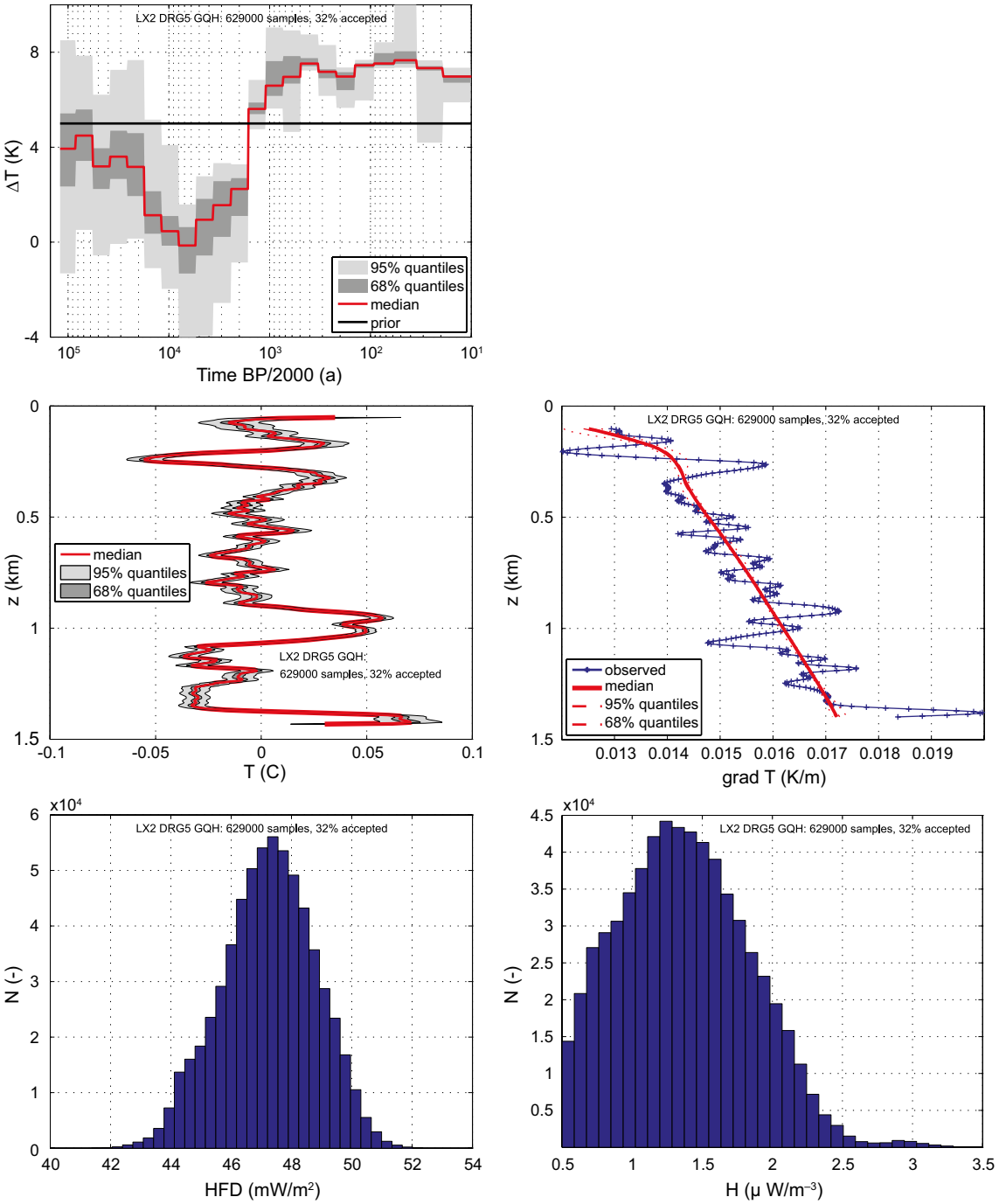

Figure 5-7. *MCMC simulations with the delayed rejection scheme of Haario et al. (2006) for the KLX02 temperature log. The estimated GSTH (top left) shows the strongest variation at 1.5–2 kyr BP, very similar to Forsmark. The data fit is good for both, temperatures (left) and the corresponding vertical gradient (right). The bottom row shows the distribution of the basal heat flow density (left) and heat production rate (right) from the KLX02 simulations, which follows a smooth distribution centred near 47 mW/m^2.*

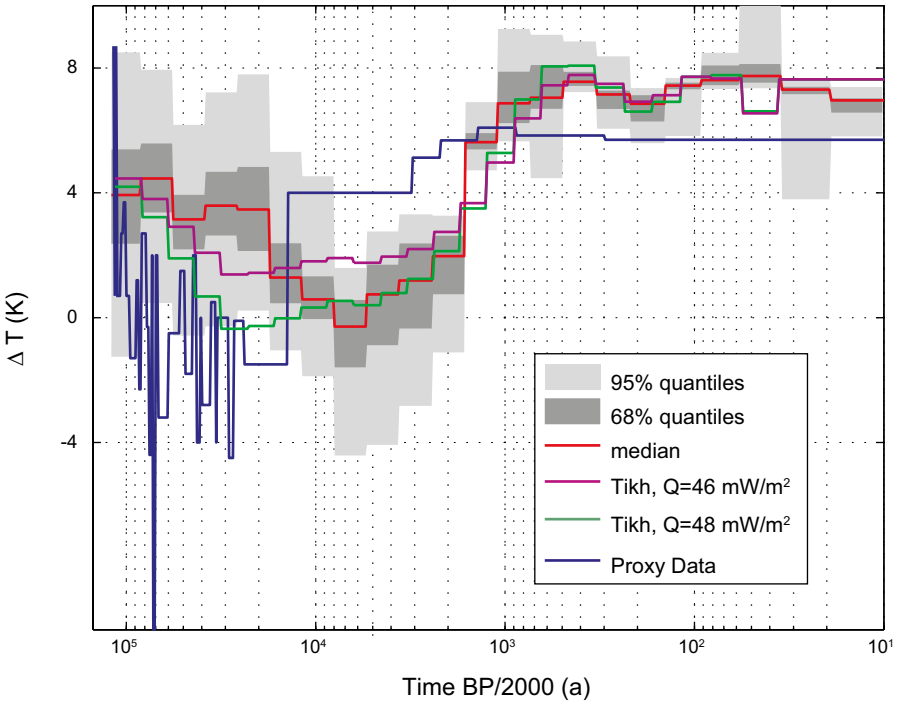

Figure 5-8. *Summary of inversion results for KLX02. The inversions from both methodologies agree well back to the last glacial maximum. However, the results presented here do not agree with the proxy data paleo-climate reconstruction (Proxy data in legend) used in Sundberg et al. (2009), see also discussion section.*

6 Discussion

From the results of the inversion studies described in the previous chapter, several questions arise, discussed below.

6.1 Depth of temperature logs

Temperature data in both target areas, Forsmark and Laxemar, only reach a depth of about 800–1 000 m (1 400 m KLX02). This does limit the validity of the results to times back to ~10 kyr BP. As argued by Rath et al. (2012), this depth is hence clearly not enough to resolve the full effect of the last glacial cycle, but at best the temperature rise after the Last Glacial Maximum. In particular, while it is possible to conclude that a temperature rise took place, the level of temperatures prior to the rise cannot be estimated from these BTPs. Furthermore, both temperature logs are ending at depths where the curvature of the temperature profile is still important. This can be seen in Figure 6-1. The results presented in Chapter 4 are in full agreement with this general observation.

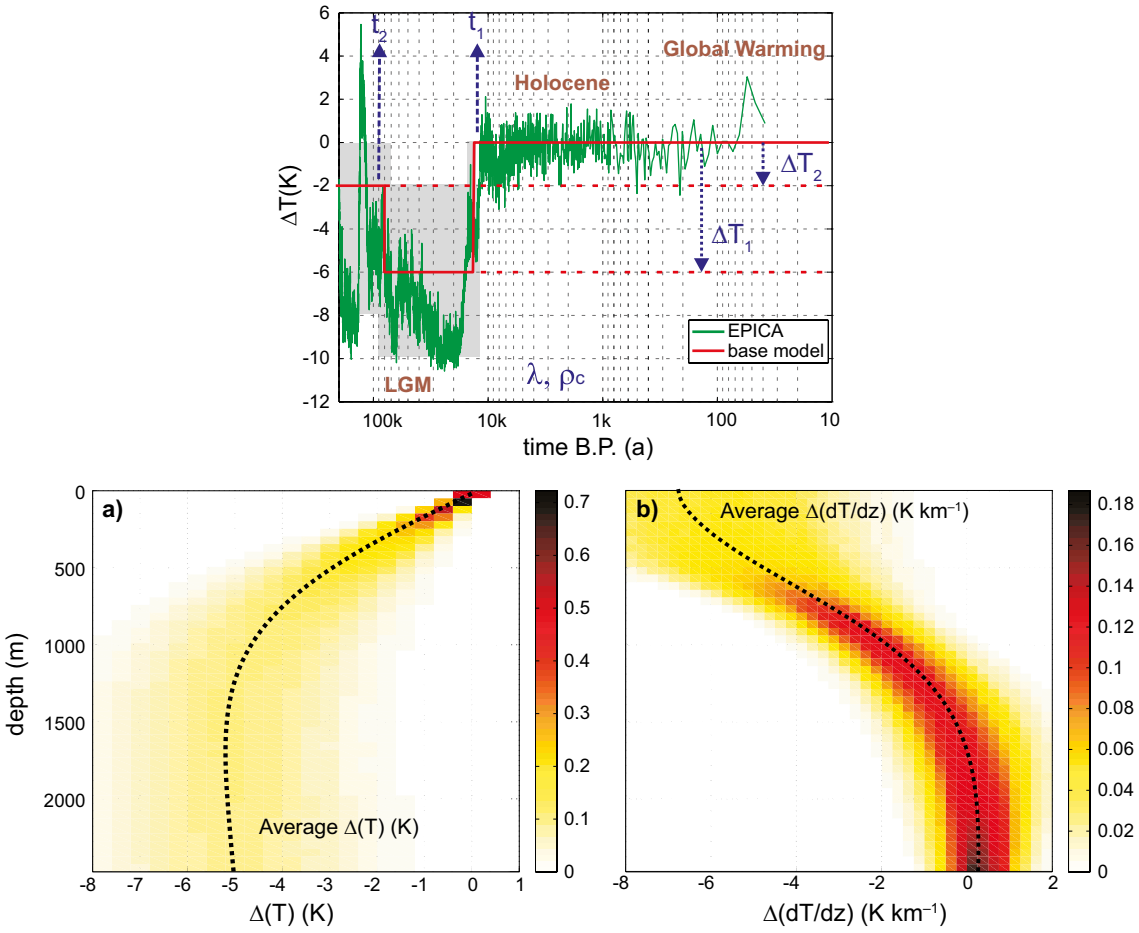

Figure 6-1. *Numerical experiments concerning the signature of the last glacial cycle in synthetic borehole temperature profiles from Rath et al. (2012). Panels (a) and (b) present the outcome of a Monte Carlo study generating samples with different values for the petrophysical properties and the assumed glacial GSTH (top panel). The colors the normalized density plot signify the number of samples for predefined cells ($\Delta z \times \Delta T$), normalized by the total number of simulations. The parameters and source code are given in the (open access) article cited above. While (a shows the resulting temperature anomaly, (b) shows the vertical gradient of temperature, which is proportional to the heat flow density.*

In order to test what can be expected from the inversions, we conducted another simple numerical experiment by using a simplified temperature reconstruction for Forsmark (SKB 2006) as used in Sundberg et al. (2009) for constructing synthetic borehole logs by forward modeling and a perturbation of these temperatures similar to the observed data. We then derived logs of lengths between 400 m and 2 400 m, which were subsequently inverted in a similar way as the observed data. The results are shown in Figure 6-2. It can easily be seen that under these assumptions, a reasonable reconstruction is possible back to the deglaciation with log lengths of about 2 000 m. Glacial and early post-glacial conditions will influence the BTP, but will not be resolvable in the inversion.

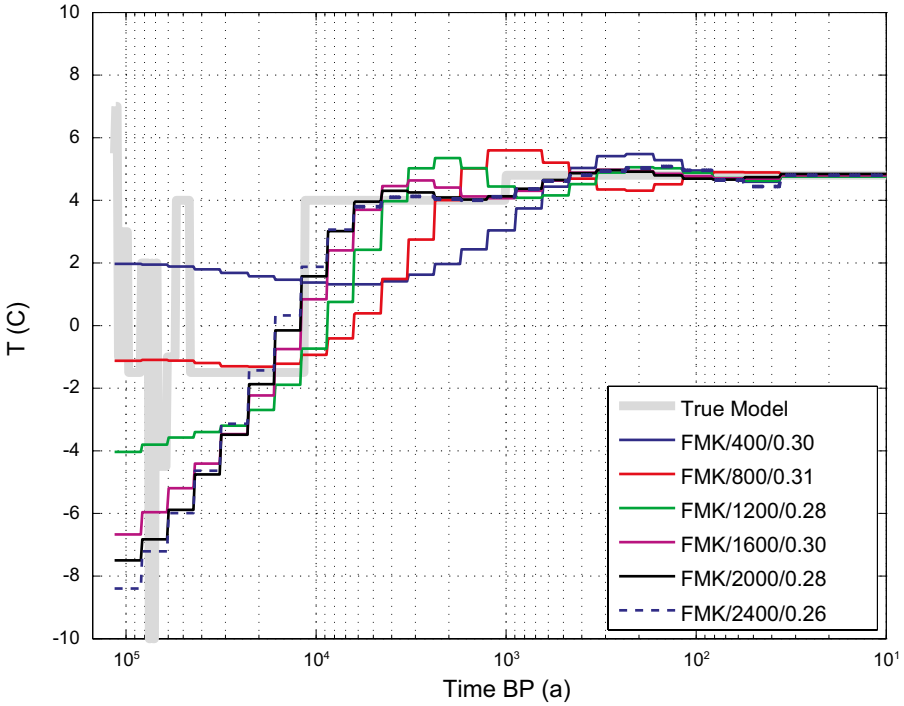

Figure 6-2. *Numerical experiment on the possible resolution of the paleoclimate reconstruction for the Forsmark site used in Sundberg et al. (2009). The proxy data paleoclimate reconstruction is shown in grey ("True Model"). All physical parameter settings were as used for the Forsmark inversions.*

6.2 Physical assumptions

As shown in many previous studies, the simplified 1D inversion applied here can produce meaningful results only if care is taken that none of the physical assumptions are violated. In general, it cannot be excluded that the heterogeneity of thermal properties may have some influence on the results. This is particularly the case in Laxemar, where strong signatures are visible in the residuals, implying that there are variations in the temperature log which cannot be explained by paleoclimate variations. This is probably caused by the mingled mineralogical composition in one of the dominant rock types in Laxemar, varying from granodioritic to quartz-monzo dioritic composition in scales from one to several hundred of meters. This is also transferred into the thermal properties causing large variability in the mentioned range of scales, see Sundberg et al. (2008b). From the results presented in Chapter 5, it appears that this is a major problem at the Laxemar KLX02 site. In Figure 6-3, the variability in thermal conductivity in the Laxemar area is visualized for some boreholes. It is obvious from the figure that these large variations in thermal conductivity have significant influence on the temperature log. The modelled thermal conductivity profile for KLX02 is available, but only down to less than 1 000 m.

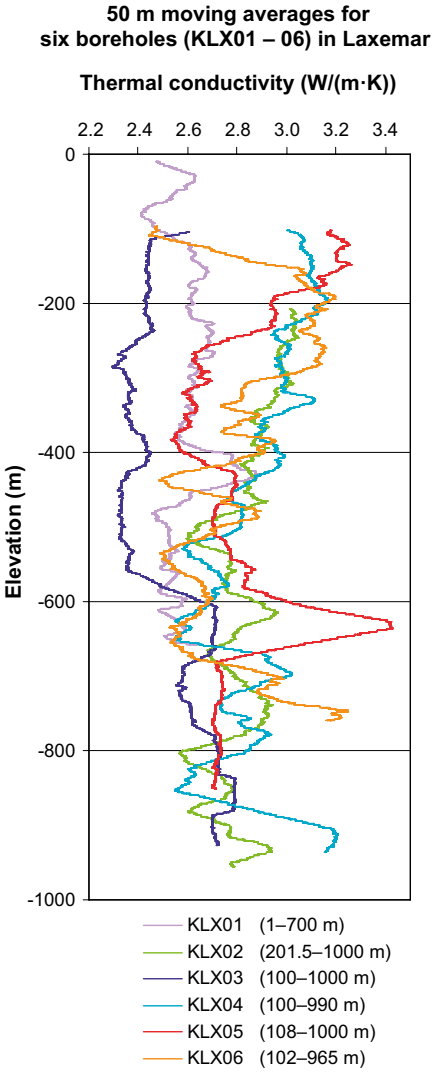

Figure 6-3. *Visualization of large-scale changes in thermal conductivity with depth for six boreholes in Laxemar, modelled from laboratory measurements, rock type distribution and density log. Thermal conductivity is expressed as moving geometrical mean over 50 meter long sections. For rock types other than "Ävrö granite", within rock spatial variability is not considered. Consequently the variability is underestimated for some borehole sections, e.g. lower parts of KLX03 and KLX05 dominated by quartz monzodiorite (Wrafter et al. 2006).*

It should also to be kept in mind that even when the observations can be fit with small deviations, it is still not guaranteed that long spatial wavelength features are not erroneously taken for a paleoclimate signal. This should be bared in mind when using the results in this report.

Nevertheless, adopting a 1D modelling approach is a useful simplification. The results, at least for Forsmark, indicate that this approach leads to meaningful results. Here, there are no strong anomalies present in the residual, and the variability found is associated with small spatial length scales. This may be taken as justification that there is no necessity to include 2D/3D effects or anisotropy in this case. In Laxemar, the situation is less clear, due to the comparatively large and structured residuals encountered here. While the principle of parsimony ("Occam's razor") speaks in favor of this simplification, further investigations based on a 3D model may challenge this assumption. Particularly interesting would be the effect of anisotropy, which cannot be included in a 1D model in a general way, but is relevant in the environment of Forsmark and Laxemar (Sundberg et al. 2009). In Laxemar it is not possible to consider anisotropy effects since the orientation varies over the area and is not consistent and therefore hard to determine. However, in Forsmark it is possible to choose an appropriate value of conductivity as in the 1D model since the orientation of anisotropy is subvertical, see Section 6.4.

Related to this problem is the question of representativeness of the laboratory measurements of the thermal rock properties. This does not only concern the choice of samples, but also the question of whether the properties in the laboratory are identical to the ones under *in situ* pressure conditions. While temperature effects are rather small, as pointed out in Section 4.1, pressure may play a role for the thermal conductivity λ, which is known to be influenced by the presence of micro-cracks or related phenomena (Hartmann et al. 2005), and would be expected in the depth interval of less than 1 000 m considered here. However, if the samples are water saturated, the pressure influence up to 50 MPa appears to be low, approximately 1–2 % according to Walsh and Decker (1966). All determinations of thermal conductivity performed in the site investigations have been made on water-saturated samples. The pressure dependence has therefore been neglected in the modelling, see e.g. SKB (2009).

An important physical effect which could possibly interfere with the borehole temperatures is fluid flow. However, no clear and direct indications of thermally relevant fluid flow at depths below approximately 100 m are found in the averaged temperature logs neither at Forsmark nor at Laxemar. Some local, small-scale effects visible in the gradients in the single logs were probably strongly reduced by the data processing during the upscaling to the computational mesh. Given the generally very low porosity (less than 1 %), we propose that the temperature logs can be considered as representing a conduction dominated heat transfer regime, and can be used for inversion.

Remaining perturbation from drilling is a reason for uncertainties in the temperature logs, see Chapter 2.

6.3 Paleoclimate

In the following we discuss some of the features found in the inversion results, going backwards in time, with emphasis on their uncertainty. In order to facilitate the discussion, we summarize the results from the present study using averaged compound temperature data from Forsmark and KLX02 in Figure 6-4. Here we combine the results from the stochastic MCMC simulations with some important time markers and relevant temperatures and the proxy reconstructions from Luterbacher et al. (2004). This chapter also includes a section where we discuss the results of the inversions using the two selected Forsmark boreholes with different known environmental history (Figure 5-5). These results are compared and discussed in terms of their individual environmental history, and specifically their timing of post-glacial transition from marine to terrestrial conditions.

6.3.1 Simulations using averaged compound temperature data

As previously mentioned, the last 100 years are not well represented in the observations, as the top 50 or even 100 m had to be neglected for the paleoclimate inversions. For this reason the GSTH for both sites stay very near their respective prior model. This means, that the climate development since the end of the Little Ice Age (AD 1350 to 1850), which is easily seen in the reconstructions from Luterbacher et al. (2004), cannot be resolved.

For the observational period, we compare our results with the paleo-temperature reconstructions for the last 500 years published by Luterbacher et al. (2004). The authors present a spatially resolved reconstruction of annual SAT, with a resolution of 0.5 degrees. The gridded values were interpolated to the borehole position by a simple inverse squared distance weighted average. A lack of agreement between the two temperature time series was to be expected, as borehole temperatures are not able to record short-term events like the anomaly found between 1700 and 1800 AD. The lack of resolution is probably not due to a "smearing" of the Forsmark signal by groundwater flow. The recent results of Trinchero et al. (2014) (see also Söderbäck 2008) indicate that there has not been vigorous vertical fluid flow in the subsurface, as some of the geochemical characteristics for different generations of groundwater still survive to the current day. In numerical permafrost simulations performed for Forsmark (Hartikainen et al. 2010) the 2D groundwater flow modelling indicated that the water flow did not advect enough heat to efficiently influence the bedrock temperature field.

With respect to the aforementioned paleo-temperature reconstructions (Luterbacher et al. 2004), the Surface Air Temperatures (SAT) derived from a set of proxies for atmospheric conditions as shown in Figure 6-4 may be considerably different from the GSTH. This is mainly an effect of conditions near the surface, which control the energy and water balance. In the area considered, these factors are dominantly vegetation, snow cover, permafrost, and possible near surface flow (Hartikainen et al. 2010). Their effect is not easily quantified for a given site for times reaching far back into the past. Assuming modern surface conditions, which may be a justified simplification for the short times of the observational period, in some cases, a particular linear SAT-GST relationship $T_{GST} = a \cdot T_{SAT} + b$ can be derived by a regression between both temperatures involved. We obtained the best general agreement with the transformation derived by Kukkonen (1987) from observations from several long term monitoring sites in Finland (coefficients a = 0.71 and b = 2.93). This linear relationship also fits data from Forsmark and Laxemar well (Figure 6-5).

The paleotemperature reconstructions (Luterbacher et al. 2004) included in Figure 6-4 were transformed using these regression coefficients. The already comparatively high temperatures between 800 and 1 800 years BP appear to be a robust feature of the inversions presented here.

The GST for the last 1 000 years broadly matches the transformed results from the reconstructions. The characteristic peak at around 250 years BP is not reproduced. This is probably because of the low resolution of the paleoclimate inversion. Though present in the proxy reconstructions for a large area in northern Europe, it could not be found in any other borehole temperature inversion, even in the ones with better data coverage as the Outokumpu scientific borehole described in Kukkonen et al. (2011a, b). However, a possible divergence of the estimates because of not yet investigated physical reasons, which are related to the underlying proxy types, cannot be excluded. The slightly higher temperatures found for early medieval times are only weakly visible in the simulation results, as they fall into the time of the smooth temperature rise from the water-covered to the terrestrial period. Another reason for not seeing the higher temperatures of the Medieval warm period relates to the methodology of here using a compound average temperature curve as input data to the inversions. For a more in-depth analysis of these effects, and the possible temperatures at Forsmark for this period of time, see Section 6.3.2.

While showing a similar development since around 2 kyr BP, the GSTHs before this time are different from each other as well as from the paleoclimate reconstruction presented in SKB (2006) and used in Sundberg et al. (2009). A remarkable common feature is the abrupt temperature rise at 1.8 – 2 kyr BP, embedded in a general smooth temperature increase (Figure 6-4). Here, the two sites show the largest differences. This temperature development, if confirmed, is not fully consistent with simple conceptions on the paleo-environmental development at the sites, and contradicts the GSTHs derived from the temperature reconstructions for both sites, as can be seen in Figure 5-4 and even more pronounced in Figure 5-8.

Obviously, given the lengths of the temperature logs and the uncertainties already mentioned above, the most important questions are (1) whether these differences between the sites are trustworthy, and (2) whether a physical explanation can be found. The key for understanding the GST development possibly lies in the geographical position of both areas. In the following, for the paleo-environmental conditions we mainly use the information on timing and duration of terrestrial conditions from Table 2-2, and information from Söderbäck (2008) and SKB (2006).

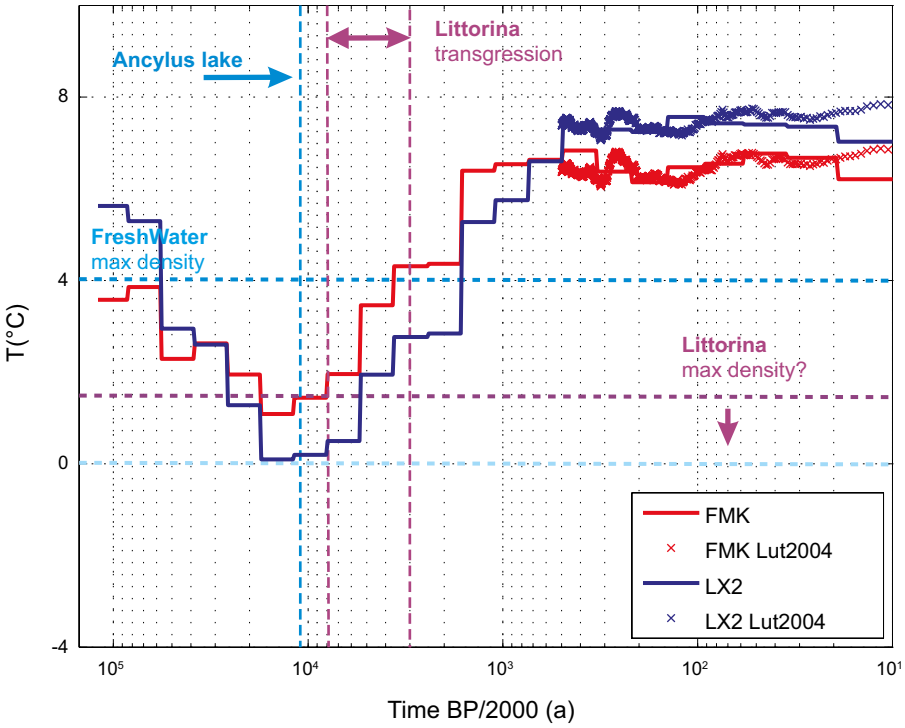

Figure 6-4. *Summary of results from the present study. The median of the Forsmark and KLX02 simulation are shown as solid lines. Some geological time intervals and temperatures (e.g., water density maximum) relevant to the text are also shown.*

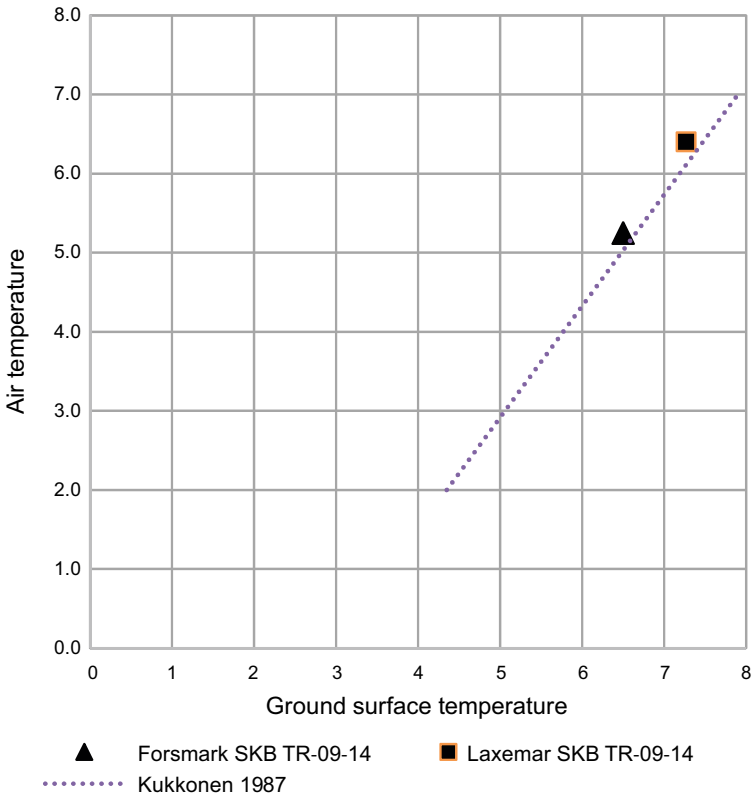

Figure 6-5. *Ground surface temperature (GST) versus air temperature. GST for Forsmark and Laxemar are extrapolated to the ground surface from the temperature logs in a number of boreholes (Sundberg et al. 2009). A linear expression from Kukkonen (1987) is shown for comparison.*

Concerning the reliability of our simulation results, the main problem is to discriminate which features are required by the data, and which are produced by the estimation procedure. This is a problem shared by any indirect estimation, and is particularly difficult in ill-posed problems as the one encountered in this study.

Both deterministic and stochastic inversions indicate that the results are reasonably reliable back to a few kyr BP, reaching possibly back to the time of deglaciation. This may be concluded from the posterior distributions in the stochastic simulations, and the very consistent behavior of the deterministic regularized inversions in this time period for both sites. From the sensitivity test shown in Figure 6-2 it is obvious that the temperatures in the depth ranges found in the studied boreholes are sensitive to paleo-temperature changes in the time period discussed here. Within an inverse framework, whenever the data do not contain sufficient information, the results will be dominated by the prior information. In the case of the deterministic inversions, this will be the smoothness enforced by the regularization method, while for the stochastic approaches the posterior parameters and their probabilities will be similar to their priors. This is the case for the behavior of the GSTH before 10 kyr BP. It has to be noted that the high temperatures at the beginning of the glacial cycle are a result of the choice of initial conditions as a result of a large number of similar cycles, as explained in Section 4.1. This behavior, though plausible, is thus a result of the prior knowledge, and is not enforced by the observations.

The physical explanation of the results, if considered trustworthy, is challenging, and necessarily speculative. The basic features to be discussed are the timing of the rise of the study areas above the sea level, and the temperature development at the ground surface during the time of water cover.

Fennoscandia has been exposed to a complex history of glaciated phases during the last (Weichselian) glacial cycle. During this period, in the Baltic area, there have been several periods of fast changes in ice sheet extension and thickness (e.g. SKB 2014a and references therein). Significant advances in the understanding of this complex history have been made in the last two decades (e.g. Siegert et al. 2001, Andrén et al. 2011, 2015, Helmens 2013, Wohlfarth 2013, Hughes et al. 2015, 2016, Stroeven et al. 2016, Stokes et al. 2015). For borehole temperatures, the dominating signatures in the depth interval considered here are the temperature change related to the deglaciation period following the LGM (including the post-glacial transition from marine to terrestrial conditions), the Holocene warm period, and the minor variations during the last two millennia. The development of the Baltic area during this period is also complex, as after the retreat of the Fennoscandian ice sheet, vast areas in e.g. Southern Sweden were submerged by the Baltic until historical times.

As can be seen in Figure 6-6, Forsmark and Laxemar were not deglaciated at the same time. The last deglaciation of Laxemar occurred at 14 kyr BP, whereas the deglaciation of Forsmark occurred some 3 kyr later, at 10.8 kyr BP (Söderbäck 2008). As previously mentioned, there are also major differences in how long time the individual boreholes within the Forsmark site have been exposed to terrestrial conditions following deglaciation and submerged conditions. The differences are up to 900 years (see Table 2-2). However, from the results of the inversion using averaged compound temperature data, discussed in the present section, no direct conclusion can be drawn on this development. The results using boreholes selected for their different known histories regarding the timing of transition from marine to terrestrial conditions, on the other hand, do provide insight to the climate development during these periods, see Section 6.3.2.

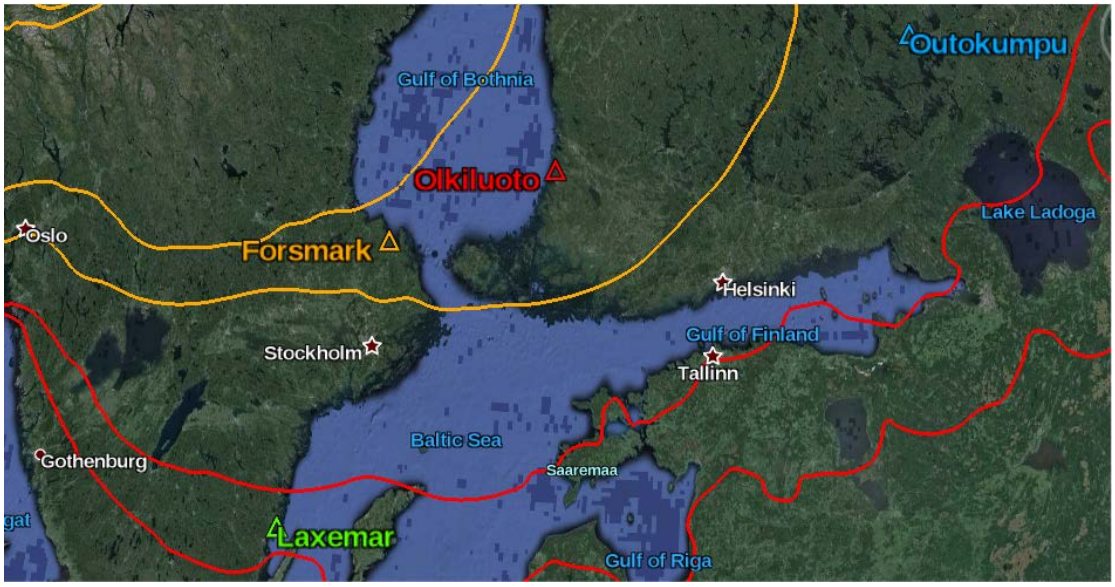

Figure 6-6. *Minimum and maximum ice cover at 11 kyr BP (yellow) and 14 kyr BP (red) in the Baltic area. This is based on the DATED-1 reconstruction Hughes et al. (2015, 2016). Laxemar was deglaciated at 14 kyr BP, about 3 kyr earlier than Forsmark.*

A first and surely too simple approach to interpret the surface temperatures for the submerged period assumed a gravity-controlled layering of the water cover. The maximum density of fresh water occurs at +4 °C, and higher salinities reduce this characteristic temperature marker. The development of the relative sea level in the Baltic is reasonably well known from many geomorphological indicators, while its salinity is still a matter of discussion, as the different proxy methods do not agree well (Andrén et al. 2011, Harff et al. 2011). Salinity affects the water density minimum temperature, and for the range of salinities considered representative for the Baltic Sea during the Holocene, its value has varied from about 2.5 °C (salinity 6 g/L) to about 1 °C (salinity 12 g/L) (IOC, SCOR, IAPSO 2010). In a stratified lake/sea environment, water salinity alone would strongly influence the temperature of the sea floor, which would be totally decoupled from the ground surface temperature on-shore. The most saline phase (the Littorina Sea) culminates in the highest relative sea level near 6 kyr BP, when the maximum salinity of 12 g/L was reached. This high-salinity period should also agree with the coldest water in contact with the ground surface. The more recent salinity history is less clear, as for the last 2 kyr there is no agreement on the general trend (Andrén et al. 2011, 2015). Moreover, the salinity deduced from averaged point measurements in the Baltic area do not represent spatial heterogeneity, and thus may not be valid for a particular environment.

The results from the paleoclimate inversions presented here are not consistent with such a simple explanation. While generally lying in the interval to be expected, i.e. between 4 °C and 1 °C, the behavior of the temperatures at Forsmark and KLX02 is complicated.

At Forsmark, the temperature in the water-covered period is systematically higher than in KLX02, and is near the freshwater maximum density temperature for the late and middle Holocene, with lower temperatures down to 1.5 °C. The paleo-environmental development shown in Söderbäck (2008) mainly shows brackish water over this period, changing smoothly from 170 m directly after the removal of the ice sheet to the rise above sea level about 2.5 kyr BP.

Could there be environmental conditions consistent with the GSTH derived from the borehole? It has to be kept in mind that the water depth in the area changed considerably reaching a very shallow estuarine environment already during the proposed salinity maximum 5 to 6 kyr BP. It has to be expected that salinity, temperature, and hence density may have been influenced by the supply of fresh water from contributing rivers and evaporation/precipitation. Large spatial and temporal gradients in salinities and temperatures probably prevailed (Valle-Levinson 2010, Omstedt 2011). Low winter temperatures at the ground surface may have been inhibited by the isolation and latent heat effects. With these conditions it can not be taken for granted that a stable layering existed and it is thus difficult to constrain the borehole results from independent reconstructions of the conditions of the water cover.

The time of rise above sea level (transition from marine to terrestrial conditions) for the individual Forsmark borehole locations that are included in the averaged compound data set occurs between ca 400 to 1 300 kyr BP (Table 2-2). These are all later than the rise to the probable SAT level derived from the inversions using the averaged compound temperature data, which is near 1.8 kyr BP. As the process of emergence occurs in a spatially heterogeneous way, and involves large changes in the surface processes which influence the surface energy balance (sedimentation and vegetation changes) a discrepancy here is not surprising. An additional reason for the discrepancy is likely to be the methodology of using averaged compound data as input to the inversions instead of individual or grouped borehole data based on their respective environmental histories. In order to get a better consistency between modelled results on GSTHs and the environmental conditions at the Forsmark site, the development at the individual drill sites need to be taken into consideration, see the following section.

In the case of KLX02, our results are difficult to reconcile with the paleo-environmental development described in Söderbäck (2008). Having been deglaciated approximately around 14 kyr BP (3 kyr earlier than Forsmark), it should have seen the full development from the Baltic Lake through the Yoldia Sea, the Ancylus Lake to modern conditions (Figure 6-7) with all the proposed salinity changes. The KLX02 drillsite emerged above sea level at around 8 465 years BP (Table 2-2). Also it has to be kept in mind that KLX02 has been in a position very near to the coastline since about 11 kyr BP. The local hydrodynamics related to fresh water supply and other environmental factors are unknown. Since then, the complicated surface conditions already mentioned above have prevailed, which includes a development from saline water cover to islands, lakes, bogs, peatland finally forest. The inversion results for Laxemar show generally lower temperatures than for Forsmark, with the largest change in temperature occurring at the same time as at Forsmark. The temperatures, though with a large uncertainty, are between 0 °C and 2.5 °C, consistent with that of brackish water at maximum density. It is not clear whether the fall of temperature since the time of deglaciation is required by the data. This behaviour of the reconstruction is however also influenced by the constraints imposed by the choice of the temporal covariance in the inversion. Stochastic and deterministic methods lead to consistent results far back into the past, in contrast to the case of Forsmark, where they agree only back to approximately 10 kyr BP.

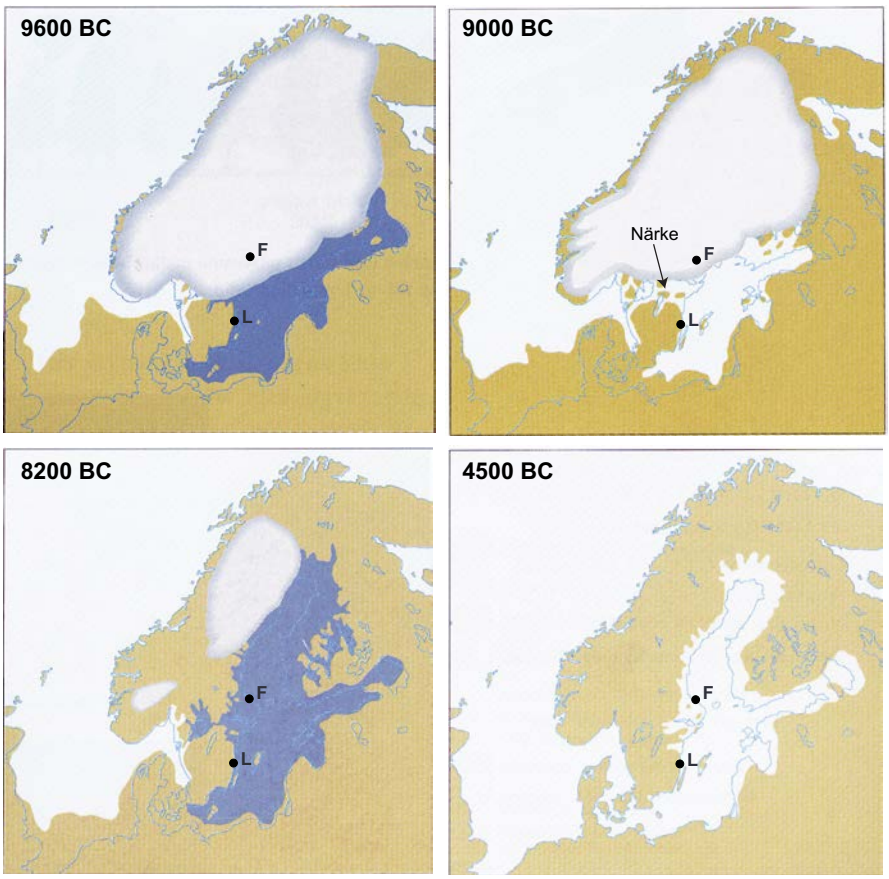

Figure 6-7. *Development of the Baltic during the last deglaciation/Holocene. Dark blue denotes the presence of fresh water, while the blueish-white indicates brackish or sea-water (Söderbäck 2008).*

6.3.2 Simulations using temperature data from boreholes with known different environmental histories

As previously mentioned, the inversion conducted using the temperature data from the two Forsmark boreholes selected to represent two groups of locations with different environmental histories, was simple and not made with optimized model parameters. Nevertheless, the tentative interpretation of the results (see Figure 5-5), i.e. that FMK02A shows a 1.5–2 degree temperature increase starting at ~1100 BP and that this signal is absent at FMK01A, is in line with the environmental development of the two drillsites as governed by isostatic rebound. KFM02A is today located at 7.26 m a.s.l. whereas KFM01A is located at 3.04 m a.s.l. (Table 2-2). Following the last deglaciation, this 4.2 m difference in elevation resulted in the KFM02 drillsite emerging from the Baltic Sea significantly earlier than the KFM01 location. At the KFM02 location, the transition from marine to terrestrial conditions occurred around 1114 BP (AD 856), whereas KFM01 continued to experience marine conditions up until around 484 BP (AD 1486) (Table 2-2). Prior to ~1100 BP, the results from the inversions show similar temperatures for the two locations (Figure 5-5). Around, or somewhat prior to, ~1100 BP, the simulated GSTH at KFM02 rises substantially and remains high for several hundreds of years. This clear temperature increase is not present at KFM01, where the GSTH remains more or less stable, and 2.5–3 degrees lower, during the same period (Figure 5-5). This is concordant with a development where KFM02 emerges from the sea at around 1100 BP, and thus starts to experience warmer temperatures (around +8 °C according to the tentative modelling results), whereas KFM01 remains submerged by the sea for another 600 years (until around 484 BP). Furthermore, since the mean bedrock thermal properties for the two drillsites are judged to be almost the same, the difference in the results may be caused by the timing of the rise above sea-level.

The *Medieval warm period* was a warm climate period between around AD 950 and 1250 with average air temperatures in Europe as high, or higher, than at present (e.g. Linderholm and Gunnarsson 2005). The above interpretation suggests that the SAT at Forsmark, as derived from the regression in Section 6.3.1, was around +7 °C around the time of the Medieval warm period,. This is ~2° warmer than the present mean annual air temperature of 5.0 °C (Table 2-1). The results also suggests that this warm climate period was recorded at KFM02 but not at KFM01 since the latter remained submerged during this time. The Medieval warm period was followed by the Little Ice Age (around AD 1 350–1 860), a period that hosted the coldest climate following the end of the Weichselian glaciation. The start of the Little Ice Age (around 600 BP) coincides approximately with the start of the declining temperatures at KFM02 that follows the period with warm climate (Figure 5-5).

While the results obtained from the boreholes grouped according to their time emergence can be interpreted in a plausible way, a few remarks seem to be unavoidable. As already seen with the BTP from Laxemar (Figure 5-6, bottom left), the assumption of constant thermal conductivity resulting from averaging may lead to spurious signal in the data. There is a close local relationship between thermal conductivity and the temperature gradient, such that spatial structures not represented in the average model (i.e. in the distribution of the thermal conductivity) may lead to apparent variation in the data. As shown in Figure 6-3 we know that spatial correlations with characteristic length of 1 to hundreds of meters are present in the Laxemar area. Furthermore, the subsurface acts as a low-pass filter the temperature signal penetrating from the surface, with a characteristic spatial cut-off changing with depth. Thus local vertical variations in thermal conductivities near the drilling site d with a spatial wavelength larger than the cut-off may bias the results of the inversion. In this case, the inversion is not able to discriminate between the potential origins of the behavior of the BTP, i.e. whether it is caused by paleoclimate or by local variations in thermal conductivity.

A synthetic example for this ambiguity is given in Figure 6-8 shows the result of inverting the data generated from the simplified GSTH shown in Figure 4-4 (top) with constant thermal conductivity perturbed by sinusoidal variations of constant amplitude but different wavelengths L_k. The results show that because of the diffusive character of heat conduction, the inversion is able to interpret (erroneously) the temperature variation caused by this heterogeneity as paleoclimate when physically possible. While it is possible to mitigate this effect, e.g., by smoothing the observations, this leads to over-smooth results. Without further information on the local heterogeneity, it can thus not be excluded that the higher variability of the GSTH of FMK2 results from the presence of local correlated variations of thermal conductivity. This once more emphasizes the necessity for deep BTPs and coincident estimates of thermal properties.

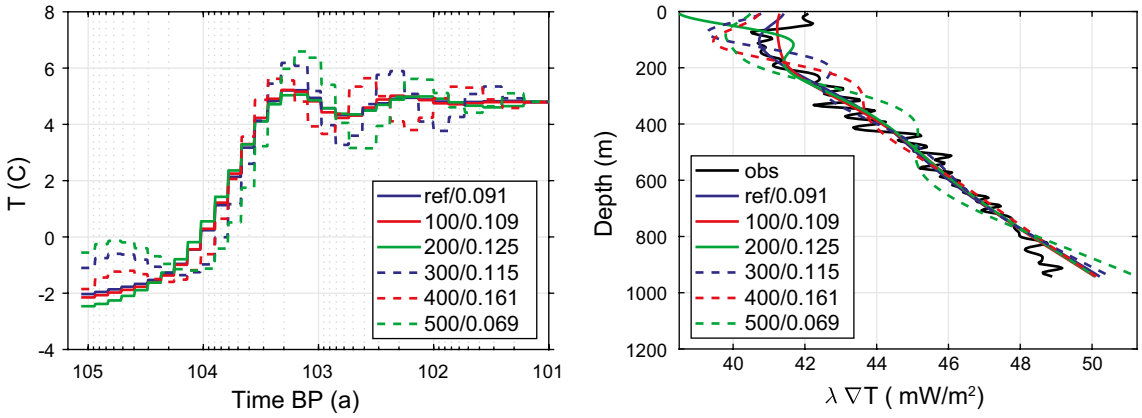

Figure 6-8. *Result of inverting the data generated from the simplified GSTH shown in Figure 4-4 (top) with additive random errors of 0.01 K. Constant thermal conductivity with sinusoidal perturbations with an amplitude of 0.1 W/(m·K) and different wavelengths L_k were assumed for the numerical experiment, which demonstrate the role of spatially correlated thermal properties.*

6.4 Comparison with heat flow from previous studies

Comparison between calculated basal heat flow between the present study and Sundberg et al. (2009) show overall good agreement, see Table 6-1.

Some small differences in the results are present, see Table 6-1, Table 1-1, Figure 5-3 and Figure 5-7. However, some minor deviations have also been discovered in the averaged input data used in the modelling in the present study compared to the earlier study by Sundberg et al. (2009), see Table 1-1, Table 4-1 and Table 4-2. The differences in data are only significant for Forsmark and are caused by non-correction for the subvertical anisotropy in thermal conductivity and small differences in heat production. Together these differences cause an overestimation of the basal heat flow at 4 000 m with approximately 4 mW/m^2 in the present study. However, these differences are not judged to influence the estimated climate data in a significant way.

When a correction is made, the suggested results on basal heat flow in this report are in excellent agreement with the modelling results in Sundberg et al. (2009), transferred to 4 000 m depth, see Table 6-1.

Table 6-1. Comparison of calculated basal heat flow at 4 000 m depth in present report and Sundberg et al. (2009).

	Basal heat flow Forsmark	**Basal heat flow Forsmark Corrected for small discrepancies in input data**	**Basal heat flow Laxemar (KLX02)**
	mW/m²	**mW/m²**	**mW/m²**
Modelling in the present report	53	49	47
Modelling in Sundberg et al. (2009)	50	50	46

7 Conclusions

There are several conclusions to be drawn from the study. From a climatological point of view, as expected, the presence of water cover following deglaciation is important at both sites. From 11 kyr BP or 14 kyr BP, for Forsmark and Laxemar, respectively, GST appear to have been between 0 °C and +4 °C until 3 kyr BP, with slightly warmer conditions (3–4 °C) at the former site and colder (near 0 °C) at the latter site. No conclusions are possible concerning the atmospheric conditions for this interval, as the influence of the water cover is not well understood. The main reason for this is the estuarine regime of shallow brackish water which probably was covering both sites until permanently rising above sea level, which must have been very sensitive to environmental change during this interval. Clearly no stable density distribution and corresponding maximum density temperature can be assumed for the water covering the sites during the postglacial period. The difference in the GSTHs for both sites may be related to the position with respect to the coastline and the particular hydrological and environmental conditions met.

The results obtained from using individual selected temperature data from two Forsmark boreholes with different environmental histories, tentatively indicate warm air temperatures of around +7 °C (that is around 2° warmer than at present) from around 1100 BP (during the Medieval warm period) for the KFM02 drill site. This coincides with the time when this borehole location had emerged from the sea. At the same time, the simulated temperature for the other borehole location (KFM01), located at a lower elevation and still submerged by water during this period, did not show this temperature increase.

Also, we find a rather clear signature of cold climate between 100 and 300 years BP associated with the Little Ice Age. For the last 500 years, the results agree well with proxy reconstructions as (Luterbacher et al. 2004), if an appropriate SAT-GST correction is applied. No indication is found in the data for the recent warming since the 19th century, which is present in the aforementioned proxy reconstruction, as well as in most other boreholes in the Northern Hemisphere. This is most likely due to the missing information in the top 100 m of the temperature logs.

Even if Forsmark constitute a site with low bedrock relief and a subtle topography, compiling bedrock temperature data from borehole locations at fundamentally different altitudes within the site, and thus with different environmental histories in terms of marine and terrestrial conditions, prohibits a detailed analysis of Holocene paleoclimate by inverse modelling. If temperature logs are available from boreholes at different elevations within a site, inverse modelling benefits a lot from the temperature records being selected and/or grouped according to their known histories/elevations. Dedicated inversions need to be done for the different groups and/or individual boreholes.

The results are compatible with a wide range of values of the basal heat flow density, influencing the paleoclimatic results only at the early periods of the GSTH where sensitivity is low (> 5 kyr BP). The joint MCMC estimations of GSTH, heat flow density, and internal heat production rate also delivers most probable basal heat flow values (4 000 m depth), which are 50 mWm^{-2} for Forsmark and 46 mWm^{-2} for Laxemar, respectively. These results support the former estimates of Sundberg et al. (2009).

It should also be noted that in general, the borehole temperature data available from the Forsmark and Laxemar sites do not represent ideal conditions for truly quantitative paleoclimate studies. The depths of the boreholes are not sufficient to reliably resolve the temperature level further back than around 10 kyr, i.e. a period basically covering the Holocene post-glacial period of the sites. Due to uncertainties in the individual temperature logs and in order to better represent respective area, new composite logs was constructed for each site either from group of logs, logs from different boreholes or from different logs in the same borehole. The use of single, equilibrated, and high quality logs combined with localized rock properties would be preferable. In addition, two single temperature logs were selected from two different Forsmark boreholes in order to represent fundamentally different environmental histories within the site.

The borehole temperature profiles from Forsmark and from the deep borehole KLX02 at Laxemar, can be inverted for ground surface temperature histories with an extraordinary (Forsmark) or at least satisfactory data fit (KLX02). In these two cases, the amplitude of the residuals is generally less than

0.05 K. As explained in Section 5.2, it was not possible to obtain satisfying results for Laxemar. The reason for this can be found in the variation in thermal conductivity for a range of scales in Laxemar. It has to be kept in mind though that a good data fit is no guarantee for realistic results on paleotemperatures. The data used here have been generated by constructing a single BTP from distinct logs, by shifting and/or averaging. In addition, the timing of the transition from marine to terrestrial conditions for the different boreholes used in this study vary significantly (between around 400 and 1 300 years BP at the Forsmark site). Furthermore, the physical bedrock properties used are averages over the full depths of different logs. Thus we cannot expect that the spatial variability in the temperature logs is fully explained, especially not in Laxemar. Furthermore, the possible effect of unresolved long-period variations appears to impact the resulting ground surface temperature models to a certain degree, reducing our confidence in these results considerably. This underlines the aforesaid necessity for high-quality logs and in situ rock properties.

Thermal conductivity data from laboratory measurements are normally in the cm scale. This is a far smaller scale compared to the relevant scale for e.g. heat flow. Through stochastic modelling of both geology and thermal properties for rock types it is possible to upscale data and spatially distribute thermal conductivities in large volumes, for instance along a borehole (e.g. Back et al. 2007, Sundberg et al. 2008b).

New deep reliable temperature log and good spatial thermal conductivity data, would make it possible to evaluate the surface temperature development for periods prior to 10 kyr BP and significant decrease uncertainties in the whole period.

8 Recommendations

In order to improve the evaluation of the ground surface temperature development, the following is recommended:

1. To improve data quality in existing boreholes and significantly reduce uncertainties, new temperature data and spatial thermal conductivity distribution along boreholes are needed.
2. New deeper boreholes are necessary in Forsmark to permit modelling of reliable ground temperature history that covers the past ice age.

Table 8-1. Recommendations for future work in Forsmark and Laxemar.

Possible actions to improve data	Forsmark	Laxemar
Existing boreholes	**Up to 1 000 m depth**	**Up to 1 700 m depth**
Temperature log	New temperature log in eg. KFM01A-02A, preferable DTS-technique with inflatable liner	Evaluate the quality of temperature measurements measured made with Posiva flow log in KLX02. Alternative: new DTS-log
Spatial thermal conductivity data	Spatial distributed data through stochastic modelling of thermal conductivity (Back et al. 2007) Alternative: Incorporate a heating wire with the DTS fibre that may enable distributed thermal conductivity measurements of sufficient quality	Extend and improve the thermal conductivity modelling along the whole borehole length (Wrafter et al. 2006) with stochastic technique (Sundberg et al. 2008b) Alternative: DTS log and possible distributed thermal conductivity measurements
Heat production	Complementary determination from core samples	Complementary determination from core samples
New deep borehole	**Up to 2 000 m**	
	New borehole or extension of the depth of existing 1 000 m deep boreholes	-
Temperature log	See above	-
Spatial thermal conductivity data	See above	-

To improve temperature data quality in Forsmark in existing boreholes it is possible to perform new high quality temperature loggings. This is possible to perform with conventional technique. However, SKB have used DTS-technique (Distributed Temperature Sensing) with optical fibre in a borehole in the GAP-project at Greenland (Harper et al. 2016, Claesson Liljedahl et al. 2016) with good experiences gained. SKB is interested in the technique for several reasons. Demonstrations and tests in Forsmark are on-going. The optical fibre can be installed with an inflatable liner that seals the borehole and prevent water movements. Repeated DTS-loggings can be made until satisfactory undisturbed conditions are achieved.

The uncertainties in the thermal conductivity are smaller in Forsmark compared to Laxemar. However, in order to gain the spatial distributed thermal conductivity and further improve the data quality, it is recommended to model the thermal conductivity along the borehole in a similar way as in the thermal site descriptive model for Forsmark 2.2 (Back et al. 2007), but conditioned instead of unconditioned. If optical fibre is installed for utilisation of distributed temperature sensing technique (DTS) it is recommended to use an optical fibre that includes a heating wire to allow controlled heating. Together with inflatable liner it then seems to be possible to determine the thermal conductivity with a resolution up to approximately 0.1 m. However, the technique first need to be developed further, tested and the results verified.

Deeper boreholes are necessary at Forsmark in order to get deep data to permit reliable inversion of the ground surface temperature history during the last ice glacial. New deep boreholes may be drilled or extension of existing 1 000 m deep boreholes may be performed.

The deepest borehole in Laxemar is the 1 700 m deep KLX02, used in the present study. The temperature logs used from KLX02 in the present study have significant uncertainties and possible biases. However, newly found additional temperature logs, made with Posiva flow log (PFL) with built-in temperature sensor of high quality, could make it possible to do further evaluations and reduce uncertainties. To take into account the large variations of thermal conductivity in a number of scales, it is possible to model the thermal conductivity distribution along the borehole for KLX02. This has already been performed for the first approximately 950 m in the thermal site descriptive model for Laxemar 2.1 (Wrafter et al. 2006) but might be possible to extend and improve with later developed stochastic modeling of lithology and thermal conductivity distribution for each rock type.

References

SKB's (Svensk Kärnbränslehantering AB) publications can be found at www.skb.com/publications.

Alexandersson H, Eggertsson Karlström C, 2001. Temperaturen och nederbörden i Sverige 1961–1990. Referensnormaler – utgåva 2. Norrköping: SMHI. (Meteorologi 99) (In Swedish.)

Andrén T, Björck S, Andrén E, Conley D, Zillén L, Anjar J, 2011. The Development of the Baltic Sea Basin During the Last 130 ka. In Harff J, Björck S, Hoth P (eds). The Baltic sea basin. Berlin: Springer, 75–97.

Andrén T, Jørgensen B B, Cotterill C, Green S, Andrén E, Ash J, Bauersachs T, Cragg B, Fanget A-S, Fehr A, Granoszewski W, Groeneveld J, Hardisty D, Herrero-Bervera E, Hyttinen O, Jensen J B, Johnson S, Kenzler M, Kotilainen A, Kotthoff U, Marshall I P G, Martin E, Obrochta S, Passchier S, Quintana-Krupinski N, Riedinger N, Slomp C, Snowball I, Stepanova A, Strano S, Torti A, Warnock J, Xiao N, Zhang R, 2015. Expedition 347 summary. Proceedings of the Integrated Ocean Drilling Program 347. doi:10.2204/iodp.proc.347.101.2015

Aster R, Borchers B, Thurber C, 2013. Parameter estimation and inverse problems. San Diego CA, Academic Press.

Back P-E, Wrafter J, Sundberg J, Rosén L, 2007. Thermal properties. Site descriptive modelling Forsmark – stage 2.2. SKB R-07-47, Svensk Kärnbränslehantering AB.

Beck A E, 1977. Climatically perturbed temperature gradients and their effect on regional and continental heat-flow means. Tectonophysics 41, 17–39.

Beck A E, 1982. Precision logging of temperature gradients and the extraction of past climate. Tectonophysics 83, 1–11.

Bellman R, 1961. Adaptive control processes: a guided tour. Princeton, NJ: Princeton University Press.

Beltrami H, Mareschal J-C, 1992. Ground surface temperature histories for central and eastern Canada from geothermal measurements: Little Ice Age signature. Geophysical Research Letters 19, 689–692.

Beltrami H, Cheng L, Mareschal J-C, 1997. Simultaneous inversion of borehole temperature data for determination of ground temperature history. Geophysical Journal International 129, 311–318.

Benfield A E, 1939. Terrestrial heat flow in Britain. Proceedings of the Royal Society A, Mathematical, Physical and Engineering Sciences 173, 428–450.

Birch F, 1948. The effects of Pleistocene climatic variations upon geothermal gradients. American Journal of Science 246, 729–760.

Bodri L, Čermák V, 2007. Borehole climatology: a new method how to reconstruct climate. Amsterdam: Elsevier.

Carslaw H S, Jaeger J C, 1959. Conduction of heat in solids. Oxford: Oxford University Press.

Čermák V, 1971. Underground temperature and inferred climatic temperature of the past millenium. Palaeogeography, Palaeoclimatology, Palaeoecology 10, 1–19.

Claesson Liljedahl L, Kontula A, Harper J, Näslund J-O, Selroos J-O, Pitkänen P, Puigdomenech I, Hobbs M, Follin S, Hirschorn S, Jansson P, Kennell L, Marcos N, Ruskeeniemi T, Tullborg E-L, Vidstrand P, 2016. The Greenland Analogue Project: Final report. SKB TR-14-13, Svensk Kärnbränslehantering AB.

Demezhko D Y, Shchapov V A, 2001. 80 000 years ground surface temperature history inferred from the temperature depth log measured in the superdeep hole SG-4 (the Urals, Russia). Global and Planetary Change 29, 219–230

Demezhko D Y, Gornostaeva A A, Tarkhanov G V, Esipko O A, 2013. 30 000 years of ground surface temperature and heat flux changes in Karelia reconstructed from borehole temperature data. Bulletin of Geography – Physical Geography Series 6, 7–25.

Farquharson C G, Oldenburg D W, 2004. A comparison of automatic techniques for estimating the regularization parameter in non-linear inverse problems. Geophysical Journal International 156, 411–425.

Gelman A, Carlin J B, Stern H S, Rubin D B, 1995. Bayesian data analysis. London: Chapman & Hall.

González-Rouco J F, Beltrami H, Zorita E, Stevens M B, 2009. Borehole climatology: a discussion based on contributions from climate modeling. Climate of the Past 5, 97–127.

Haario H, Laine M, Mira A, Saksman E, 2006. DRAM: Efficient adaptive MCMC. Statistics and Computing 16, 339–354.

Hadamard J, 1923. Lectures on the Cauchy's problem in linear partial differential equations. New Haven, CT: Yale University Press.

Hansen P C, 1998. Rank deficient and discrete ill-posed problems. Philadelphia PA: Society for Industrial and Applied Mathematics.

Hansen P C, 2010. Discrete inverse problems: insight and algorithms. Philadelphia PA: Society for Industrial and Applied Mathematics.

Harff J, Björck S, Hoth P (eds), 2011. The Baltic sea basin. Berlin: Springer.

Harper J, Hubbard A, Ruskeeniemi T, Claesson Liljedahl L, Kontula A, Brown J, Dirkson A, Dow C, Doyle S, Drake H, Engström J, Fitzpatrick A, Follin S, Frape S, Graly J, Hansson K, Harrington J, Henkemans E, Hirschorn S, Hobbs M, Humphrey N, Jansson P, Johnson J, Jones G, Kinnbom P, Kennell L, Klint K E S, Liimatainen J, Lindbäck K, Meierbachtol T, Pere T, Pettersson R, Tullborg E-L, van As D, 2016. The Greenland Analogue Project: Data and processes. SKB R-14-13, Svensk Kärnbränslehantering AB.

Hartikainen J, Kouhia R, Wallroth T, 2010. Permafrost simulations at Forsmark using a numerical 2D thermo-hydro-chemical model. SKB TR-09-17, Svensk Kärnbränslehantering AB.

Hartmann A, Rath V, Clauser C, 2005. Thermal conductivity from core and well log data. International Journal of Rock Mechanics and Mining Sciences 42, 1042–1055.

Hastings W K, 1970. Monte Carlo sampling methods using Markov chains and their applications. Biometrika 57, 97–109.

Hedenström A, Risberg J, 2003. Shore displacement in northern Uppland during the last 6 500 calender years. SKB TR-03-17, Svensk Kärnbränslehantering AB.

Helmens K, 2013. The last interglacial-glacial cycle (MIS 5-2) re-examined based on long proxy records from central and northern Europe. SKB TR-13-02, Svensk Kärnbränslehantering AB.

Hughes A L C, Gyllencreutz R, Lohne Ø S, Mangerud J, Svendsen J I, 2015. DATED-1: compilation of dates and time-slice reconstruction of the build-up and retreat of the last Eurasian (British-Irish, Scandinavian, Svalbard-Barents-Kara Seas) Ice Sheets 40-10 ka. Department of Earth Science, University of Bergen and Bjerknes Centre for Climate Research, Dataset #848117. doi:10.1594/PANGAEA.848117

Hughes A L C, Gyllencreutz R, Lohne Ø S, Mangerud J, Svendsen J I, 2016. The last Eurasian ice sheets – a chronological database and time-slice reconstruction, DATED-1. Boreas 45. doi:10.1111/bor.12142

IOC, SCOR, IAPSO, 2010: The international thermodynamic equation of seawater – 2010: Calculation and use of thermodynamic properties. Intergovernmental Oceanographic Commission, UNESCO. (Manuals and Guides 56)

Jessop A M, 1971. The distribution of glacial perturbation of heat flow in Canada. Canadian Journal of Earth Sciences 8, 162–166.

Kukkonen I, 1987. Vertical variation of apparent and palaeoclimatically corrected heat flow densities in the central Baltic Shield. Journal of Geodynamics 8, 33–53.

Kukkonen I T, Jõeleht A, 2003. Weichselian temperatures from geothermal heat flow data. Journal of Geophysical Research: Solid Earth 108. doi:10.1029/2001JB001579

Kukkonen I T, Šafanda J, 1996. Palaeoclimate and structure: the most important factors controlling subsurface temperatures in crystalline rocks. A case history from Outokumpu, eastern Finland. Geophysical Journal International 126, 101–112.

Kukkonen I T, Rath V, Kivekäs L, Šafanda J, Čermak V, 2011a. Geothermal studies of the Outokumpu Deep Drill Hole, Finland: Vertical variation in heat flow and paleoclimatic implications. Physics of the Earth and Planetary Interiors 188, 9–25.

Kukkonen I, Kivekäs L, Vuoriainen S, Kääriä M, 2011b. Thermal properties of rocks in Olkiluoto: Results of laboratory measurements 1994–2010. Posiva Working Report 2011-17, Posiva Oy, Finland.

Kukkonen I T, Rath V, Korpisalo A, 2015. Paleoclimatic inversion of ground surface temperature history from geothermal data on the Olkiluoto drill hole OL-KR56. Posiva Working Report 2015-49, Posiva Oy, Finland.

Lachenbruch A H, Marshall B V, 1986. Changing climate: geothermal evidence from permafrost in the Alaskan Arctic. Science 234, 689–696.

Lachenbruch A H, Sass J H, Marshall B V, Moses T H 1982. Permafrost, heat flow, and the geothermal regime at Prudhoe Bay, Alaska. Journal of Geophysical Research: Solid Earth 87, 9301–9316.

Linderholm H W, Gunnarson B E, 2005. Summer temperature variability in central Scandinavia during the last 3 600 years. Geografiska Annaler 87A, 231–241.

Luterbacher J, Dietrich D, Xoplaki E, Grosjean M, Wanner H, 2004. European seasonal and annual temperature variability, trends and extremes since 1500. Science 303, 1499–1503.

Mareschal J-C, Rolandone F, Bienfait G, 1999. Heat flow variations in a deep borehole near Sept-Iles, Quebec, Canada: Palaeoclimatic interpretation and implications for regional heat flow estimates. Geophysical Research Letters 26, 2049–2052.

Metropolis N, Rosenbluth A W, Rosenbluth M N, Teller A H, 1953. Equations of state calculations by fast computing machines. Journal of Chemical Physics 21, 1087–1092.

Mosegaard K, Tarantola A, 1995. Monte Carlo sampling of solutions to inverse problems. Journal of Geophysical Research 100, 12431–12447.

Mosegaard K, Tarantola A, 2002. Probabilistic approach to inverse problems. In Lee W, Jennings P, Kisslinger C, Kanamori H (eds). International handbook of earthquake and engineering seismology, Part A, Volume 81A. San Diego, CA: Academic Press, 237–265.

Mottaghy D, 2007. Heat transfer processes in the upper crust: influence of structure, fluid flow, and palaeoclimate. PhD thesis. Rheinisch-Westfälische Technische Hochschule, Aachen, Germany.

Mottaghy D, Rath V, 2006. Latent heat effects in subsurface heat transport modeling and their impact on paleotemperature reconstructions. Geophysical Journal International 164, 236–245.

Mottaghy D, Schellschmidt R, Clauser C, Kukkonen I T, Nover G, Milanovsky S, Romushkevich R A, 2005. Popov Y A, New heat flow data from the immediate vicinity of the Kola superdeep borehole: Vertical variation in heat flow density confirmed. Tectonophysics 401, 119–142.

Omstedt A, 2011. Guide to process based modeling of lakes and coastal seas. Berlin: Springer.

Patankar S V, 1980. Numerical heat transfer and fluid flow. Philadelphia, PA: Hemisphere.

Posiva, 2012. Olkiluoto Site Description 2011. Posiva 2011-02, Posiva Oy, Finland.

Påsse T, 2001. An empirical model of glacio–isostatic movements and shore level displacement in Fennoscandia. SKB R-01-41, Svensk Kärnbränslehantering AB.

Rath V, Mottaghy D, 2007. Smooth inversion for ground surface temperature histories: estimating the optimum regularization parameter by generalized cross-validation. Geophysical Journal International 171, 1440–1448.

Rath V, González-Rouco J F, Goosse H, 2012. Impact of postglacial warming on borehole reconstructions of last millennium temperatures. Climate of the Past 8, 1059–1066.

Shen P Y, Beck A E, 1991. Least squares inversion of borehole temperature measurements in functional space. Journal of Geophysical Research 96, 19965–19979.

Siegert M J, Dowdeswell J A, Hald M, Svendsen J-I, 2001. Modelling the Eurasian Ice Sheet through a full (Weichselian) glacial cycle. Global and Planetary Change 31, 367–385.

SKB, 2006. Climate and climate-related issues for the safety assessment SR-Can. SKB TR-06-23, Svensk Kärnbränslehantering AB.

SKB, 2008. Site description of Forsmark at completion of the site investigation phase. SDM-Site Forsmark. SKB TR-08-05, Svensk Kärnbränslehantering AB.

SKB, 2009. Site description of Laxemar at completion of the site investigation phase. SDM-Site Laxemar. SKB TR-09-01, Svensk Kärnbränslehantering AB.

SKB, 2010. Climate and climate-related issues for the safety assessment SR-Site. SKB TR-10-49, Svensk Kärnbränslehantering AB.

SKB, 2011. Long-term safety for the final repository for spent nuclear fuel at Forsmark. Main report of the SR-Site project. SKB TR-11-01, Svensk Kärnbränslehantering AB.

SKB, 2014a. Climate and climate-related issues for the safety assessment SR-PSU. SKB TR-13-05, Svensk Kärnbränslehantering AB.

SKB, 2014b. Safety analysis for SFR. Long-term safety. Main report for the safety assessment SR-PSU. SKB TR-14-01, Svensk Kärnbränslehantering AB.

Stokes C R, Tarasov L, Blomdin R, Cronin T M, Fisher T G, Gyllencreutz R, Hättestrand C, Heyman J, Hindmarsh R C, Hughes A L, Jakobsson M, Kirchner N, Livingstone S J, Margold M, Murton J B, Noormets R, Peltier W R, Peteet D. M, Piper D J, Preusser F, Renssen H, Roberts D H, Roche D M, Saint-Ange F, Stroeven A P, Teller J T, 2015. On the reconstruction of palaeo-ice sheets: Recent advances and future challenges. Quaternary Science Reviews 125, 15–49.

Stroeven A P, Hättestrand C, Kleman J, Heyman J, Fabel, D, Fredin O, Goodfellow B W, Harbor, J. M, Jansen, J. D, Olsen L, Caffee M W, Fink D, Lundqvist J, Rosqvist G C, Strömberg B, Jansson K N, 2016. Deglaciation of Fennoscandia. Quaternary Science Reviews 147, 91–121.

Sundberg J, Wrafter J, Ländell M, Back P-E, Rosén L, 2008a. Thermal properties Forsmark. Modelling stage 2.3: Complementary analysis and verification of the thermal bedrock model, stage 2.2. SKB R-08-65, Svensk Kärnbränslehantering AB.

Sundberg J, Wrafter J, Back P-E, Rosén L, 2008b. Thermal properties Laxemar. Site description modelling. SDM-Site Laxemar. SKB R-08-61, Svensk Kärnbränslehantering AB.

Sundberg J, Back P-E, Sundberg A, 2009. Modelling of temperature in deep boreholes and evaluation of geothermal heat flow at Forsmark and Laxemar. SKB TR-09-14, Svensk Kärnbränslehantering AB.

Söderbäck B (ed), 2008. Geological evolution, palaeoclimate and historical development of the Forsmark and Laxemar-Simpevarp areas. Site descriptive modelling. SDM-Site. SKB R-08-19, Svensk Kärnbränslehantering AB.

Tarantola A, 2005. Inverse problem theory and methods for model parameter estimation. Philadelphia PA: Society for Industrial and Applied Mathematics.

Tarantola A, Valette B, 1982a. Generalized nonlinear inverse problems solved using the least squares criterion. Reviews of Geophysics 20, 219–232.

Tarantola A, Valette B, 1982b. Inverse problem = quest for information. Journal of Geophysics 50, 159–170.

Trinchero P, Delos A, Molinero J, Dentz M, Pitkänen P, 2014. Understanding and modelling dissolved gas transport in the bedrock of three Fennoscandian sites. Journal of Hydrology 512, 506–517.

Valle-Levinson A (ed), 2010. Contemporary issues in estuarine physics. New York: Cambridge University Press.

Vogel C R, 2002. Computational methods for inverse problems. Philadelphia PA: Society for Industrial and Applied Mathematics.

Wahba G, 1990. Spline models for observational data. Philadelphia PA: Society for Industrial and Applied Mathematics.

Walsh J B, Decker E R, 1966. Effect of pressure and saturating fluid on the thermal conductivity of compact rock. Journal of Geophysical Research 71, 3053–3061.

Wohlfarth B, 2013. A review of Early Weichselian climate (MIS 5d-a) in Europe. SKB TR-13-03, Svensk Kärnbränslehantering AB.

Wrafter J, Sundberg J, Ländell M, Back P-E, 2006. Thermal modelling. Site descriptive modelling. Laxemar – stage 2.1. SKB R-06-84, Svensk Kärnbränslehantering AB.

Appendix 1

Deterministic inversion approach (Tikhonov techniques)

For the deterministic approach we seek to minimize an objective function θ with respect to a given model specified by a set of parameters $\boldsymbol{m} = [m_1, m_2, \ldots m_M]$, which is defined by:

$$\theta = \left(\mathbf{d} - \mathbf{g}(\mathbf{m})\right)^T \mathbf{W}_d^T \mathbf{W}_d \left(\mathbf{d} - \mathbf{g}(\mathbf{m})\right) + R\left(\mathbf{m} - \mathbf{m}_a\right), \tag{A1-1}$$

where $\boldsymbol{W_d}$ denotes a weighting matrix commonly used to standardize the residuals $\boldsymbol{r = d - g(m)}$, i.e. it is set to the inverse square root of the data covariance matrix $\boldsymbol{C_d}$. In Equation (A1-1), the first term measures the data fit, while the second, $\boldsymbol{R(m)}$, is necessary to stabilize the generally ill-posed inverse problem, see Aster et al. (2013).

In the problem treated here, the parameter vector m is composed of a piecewise constant function of time, using a logarithmic spacing. The data vector $\boldsymbol{d} = H(\boldsymbol{d}_{obs})$ contains the result of an observation operator H applied to the discrete values of temperature measured in in the borehole. In this case, the application of this operator refers to the "upscaling" procedures mentioned later.

This regularization in Equation (A1-1) can be achieved in many different ways. Most of the results presented here use a generalized Tikhonov technique, formulating the corresponding term as:

$$R\left(\mathbf{m} - \mathbf{m}_a\right) = \tau_0 \left(\mathbf{m} - \mathbf{m}_a\right)^T \left(\mathbf{m} - \mathbf{m}_a\right) + \sum\nolimits_k \tau_k \left(\mathbf{m} - \mathbf{m}_a\right)^T \mathbf{W}_k^T \mathbf{W}_k \left(\mathbf{m} - \mathbf{m}_a\right). \tag{A1-2}$$

In this equation, we define $\mathbf{W}_k$ to be a discrete approximation to the first or second derivative of the parameters with respect to logarithmic time, see Aster et al. (2013), which can be written in discrete form using a logarithmic time step Δ:

$$\mathbf{W}_1 = \frac{1}{\Delta}\begin{bmatrix} -1 & 1 & & \cdots & & 0 \\ & -1 & 1 & & & \\ \vdots & & \ddots & & & \vdots \\ & & & -1 & 1 & \\ 0 & & \cdots & & -1 & 1 \end{bmatrix} \quad \mathbf{W}_2 = \frac{1}{\Delta^2}\begin{bmatrix} -2 & 1 & & \cdots & & 0 \\ 1 & -2 & 1 & & & \\ \vdots & & \ddots & & & \vdots \\ & & 1 & -2 & 1 & \\ 0 & & \cdots & 1 & -2 & 1 \end{bmatrix}, \tag{A1-3}$$

Taking the derivative of Equation (A1-1), and imposing the minimum conditions leads to the iteration:

$$\left(\mathbf{J}_w^T \mathbf{J}_w + \sum_{i=0}^{1} \tau_i \mathbf{W}_{m,i}^T \mathbf{W}_{m,i}\right) \delta\mathbf{m}_k = \mathbf{J}_w^T \left[\mathbf{d} - \mathbf{g}(\mathbf{m}_k)\right] - \sum_{i=0}^{1} \tau_i \mathbf{W}_{m,i}^T \mathbf{W}_{m,i} (\mathbf{m}_k - \mathbf{m}_a) \tag{A1-4}$$

$$\mathbf{m}_{k+1} = \mathbf{m}_k + \mu\delta\mathbf{m}_k.$$

We define the weighted Jacobian or sensitivity matrix as:

$$\mathbf{J}_w \equiv \mathbf{W}_d \mathbf{J} = \mathbf{W}_d \partial\mathbf{g} / \partial\mathbf{m}, \tag{A1-5}$$

and the Generalized Inverse as:

$$\mathbf{J}_w^{\dagger} = \left(\mathbf{J}_w^T \mathbf{J}_w + \sum_{i=0}^{1} \tau_i \mathbf{W}_{m,i}^T \mathbf{W}_{m,i}\right)^{-1} \mathbf{J}_w^T \ , \tag{A1-6}$$

respectively. Note that the inverse in Equation (A1-6) is the posterior covariance matrix. These quantities are appropriate tools to further analyze the sensitivity of given data to the inverse parameters.

Given the two regularization parameters τ_0 and τ_1, this formulation can be seen an approximation to an inverse spatial exponential covariance a logarithmic scale with given error and correlation length (Tarantola 2005). For the inversions shown below, τ_0 is set to a fixed small value (0.003), while τ_1 is

set to an optimal value determined by Generalized Cross Validation (GCV) (Rath and Mottaghy 2007, Farquharson and Oldenburg 2004, Wahba1990). This optimal value is found by minimizing the GCV function over a set of predefined values of the regularization parameter *t*:

$$GCV(\tau) = \frac{N\left\|\mathbf{d} - \mathbf{g}(\mathbf{m}_\tau^k)\right\|_2^2}{\mathrm{trace}(\mathbf{I} - \mathbf{J}_w\mathbf{J}_w^\dagger)^2} = \min! \qquad \text{(A1-7)}$$

For the inversions presented here, we always used the GCV criterion. The Unbiased Predictive Risk Estimator (UPRE) criterion described in Vogel (2002) produced nearly identical results. We did not use the L-curve approach described above, as this technique is not well adapted to non-linear inverse problems, where the identification of the point of maximal curvature often leads to highly improbable results.

A useful measure for comparing the goodness-of-fit for different models is the normalized Root Mean Square Deviation (RMS) defined by:

$$RMS = \sqrt{\left(N_d - 1\right)^{-1} \sum_{j=1}^{N} \left(\frac{T_j^{obs} - T_j^{cal}}{\sigma_j} \right)^2} \qquad \text{(A1-8)}$$

where N_d is the number of observations, and the second term under the root is the sum of standardized residuals. In the case of N_d being large, and approximately Gaussian and independent data, the value should be near one. However, due to the many assumptions involved, small differences in RMS are not considered as significant, and this parameter should only be used as an indicator. In particular, all runs shown here were run with a uniform error of 0.1 K for the temperature, which is usually a reasonable estimate for this quantity. Note that this error includes not only the measurement error, which is at least one order of magnitude smaller, but also all errors related to the misspecification of the model (e.g. related to the use of average properties).

Bayesian stochastic approach (Markov Chain Monte Carlo technique)

In contrast to the deterministic approach described above, the Bayesian paradigm (see e.g. Gelman et al. 1995) aims not at a single GSTH which is optimal in a previously defined sense, but seeks to estimate the full posterior probability density function (PDF), given the prior PDF and the observational data. Detailed accounts on this approach can be found in Mosegaard and Tarantola (1995, 2002) and Tarantola (2005). In the present study we concentrate on the stochastic inversions. Deterministic inversions as described in Section 3.2.1 aim at deriving a single optimum model, which will commonly not catch the characteristics of all models compatible with the data. In contrast, the stochastic methods described in this section introduce constraints in generating a large number of models from a random set of temporally correlated models, as described below. Starting from the prior distribution by $p(\boldsymbol{m})$, and the conditional probability distribution, $p(\boldsymbol{d}|\boldsymbol{m})$, also called likelihood, which describes the probability that the data, ***d***, will be observed, given a set of parameters ***m***. Given the above prior, we then seek the conditional (posterior) distribution of the model parameter(s) given the data. We will denote this posterior probability distribution for the model parameters by $p(\boldsymbol{m}|\boldsymbol{d})$. Bayes' theorem relates prior and posterior distributions by:

$$p\left(\mathbf{m}\middle|\mathbf{d}\right) \propto p\left(\mathbf{d}\middle|\mathbf{m}\right) p\left(\mathbf{m}\right) \quad , \qquad \text{(A1-9)}$$

where the proportionality constant usually is not explicitly computed.

While it is well known that, under the restrictive assumption of Gaussian probabilities, estimators can be derived, which bear some similarity to the deterministic methods described above (Tarantola and Valette 1982a, b), the technique of choice for the Bayesian is of stochastic nature.

In this study, a Markov Chain Monte Carlo (MCMC) technique was employed. We used a variant of the well-known Metropolis-Hastings algorithm (MH) (Metropolis et al. 1953, Hastings 1970, Haario et al. 2006). The Delayed Rejection Adaptive Monte Carlo (DRAM) algorithm improves on MH i) because it samples the posterior more effectively, as the rejection of low-likelihood samples

is delayed for a predefined number of steps in the MC chain, before possibly being finally excludes, and ii) because it allows for an adaption of the prior covariance during the progress of the MC chain. We used the DRAM algorithm as implemented by Haario et al. (2006), with reduced or deactivated adaptivity in order to prevent a premature concentration of models.

There are problems with this choice in the case of an ill-posed inverse problem as the one investigated here. The meaningfulness of the results depends strongly on the reasonable choice of both prior probability density, which was chosen to be a multidimensional Gaussian distribution $N(\boldsymbol{m},\boldsymbol{s})$ which characterized by its mean vector m and covariance matrix **C**, which is updated at given intervals during the MC process. In our case however, we did not assume **C** to be diagonal, but allowed for temporal correlations in the GSTH parameters, while for the remaining parameters (Q_b, H) it was initialised with the appropriate variances.

For the parameters representing the GSTH, we introduced a Gaussian temporal covariance matrix defined as:

$$C_{i,j}^{\text{gauss}} = \sigma_i^2 \exp\left[\frac{-|t_i - t_j|^2}{2L^2}\right] \qquad \text{(A1-10)}$$

Its width is controlled by a temporal correlation length L of approximately 1/2 of a decade, which agrees with the resolution obtainable in this type of reconstruction (e.g. Demezhko and Shchapov 2001). A number of chains were started in parallel, each starting from a perturbed version of the prior which was set to the average of a GSTH derived from a Tikhonov deterministic inversion of the data set.

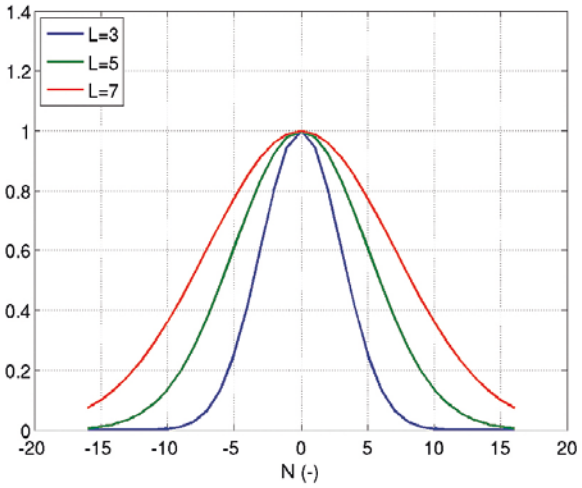

Figure A *Gaussian temporal covariances. In the MCMC samplings presented in this study, correlation lengths of 5·Δt or less were used.*

Appendix 2

Abbreviations

DTS	Distributed Temperature Sensing
FD	Finite Difference
GCV	Generalized Cross Validation
GST	Ground Surface Temperature
GSTH	Ground Surface Temperature Histories
MCMC	Markov Chain Monte Carlo
RMS	Root Mean Square Deviation
SAT	Surface Air Temperature
UPRE	Unbiased Predictive Risk Estimator

Arkitektkopia AB, Bromma, 2019

SKB is responsible for managing spent nuclear fuel and radioactive waste produced by the Swedish nuclear power plants such that man and the environment are protected in the near and distant future.

skb.se